SIAM J. Applied Dynamical Systems
Vol. 11, No. 4, pp. 1270–1309

Reduction and Dynamics of a Generalized Rivalry Network with Two Learned Patterns*

Casey Diekman†, Martin Golubitsky†, Tyler McMillen‡, and Yunjiao Wang†

Abstract. We use the theory of coupled cell systems to analyze a neuronal network model for generalized rivalry posed by H. Wilson. We focus on the case of rivalry between two patterns and identify conditions under which large networks of n attributes and m intensity levels can reduce to a model consisting of two or three cells depending on whether or not the patterns have any attribute levels in common. (The two-cell reduction is equivalent to certain recent models of binocular rivalry.) Notably, these reductions can lead to large recurrent excitation in the reduced network even though the individual cells in the original network may have none. We also show that symmetry-breaking Takens–Bogdanov (TB) bifurcations occur in the reduced networks, and this allows us to further reduce much of the dynamics to a planar system. We analyze the dynamics of the quotient systems near the TB singularity, discussing how variation of the input parameter I organizes the dynamics. This variation leads to a degenerate path through the unfolding of the TB point. We also discuss how the network structure affects recurrent excitation in the reduced networks, and the consequences for the dynamics.

Key words. neuronal networks, rivalry, coupled cell systems, Takens–Bogdanov bifurcation

AMS subject classifications. 37G15, 37G40, 34C23, 92B20

DOI. 10.1137/110858392

1. Introduction and main results.

Wilson (2009) introduced a network model for generalized rivalry between learned patterns. Specifically, the network model consists of an $m \times n$ array of *nodes* or *cells* where each column represents a pattern attribute and each row represents the intensity of that attribute in the pattern.

Certain reciprocal inhibitory and reciprocal excitatory connections are also specified in the network model. First, the cells within each attribute column have powerful reciprocal inhibitory connections. See Figure 1 (left). These connections work to prevent more than one cell in each column from firing at the same time. In this network model, a *pattern* is a choice of one node from each column, and a *learned* pattern is a pattern with reciprocal excitatory connections between all pairs of cells in different columns that correspond to that pattern. See Figure 1 (right).

The study of generalized rivalry assumes that the network has two or more learned patterns

*Received by the editors December 9, 2011; accepted for publication (in revised form) by B. Sandstede July 9, 2012; published electronically October 11, 2012.
http://www.siam.org/journals/siads/11-4/85839.html
†Mathematical Biosciences Institute, The Ohio State University, Columbus, OH 43210 (cdiekman@mbi.osu.edu, mg@mbi.osu.edu, ywang@mbi.osu.edu). This research was supported in part by NSF grant DMS-1008412 to the second author and NSF grant DMS-0931642 to the Mathematical Biosciences Institute. The work of the fourth author was partially supported by Rice University.
‡Department of Mathematics, California State University at Fullerton, Fullerton, CA 92834 (tmcmillen@fullerton.edu). This author's work was partially supported by the Mathematical Biosciences Institute.

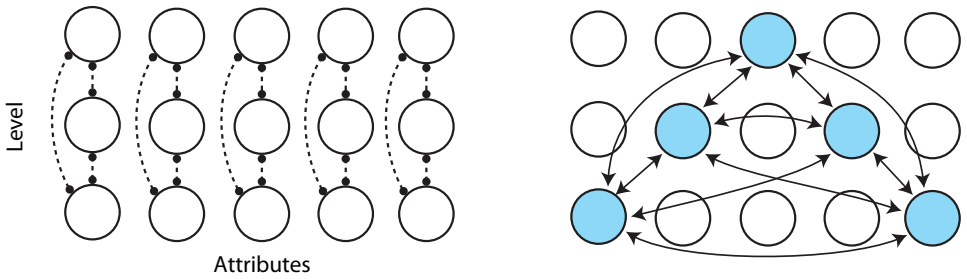

Figure 1. *Network model for generalized rivalry. Each column represents an attribute, whereas each row represents a level of that attribute. Left: Dashed lines indicate reciprocal inhibitory connections between all cells in a column. Right: Solid lines indicate reciprocal excitatory connections between cells in a given learned pattern.*

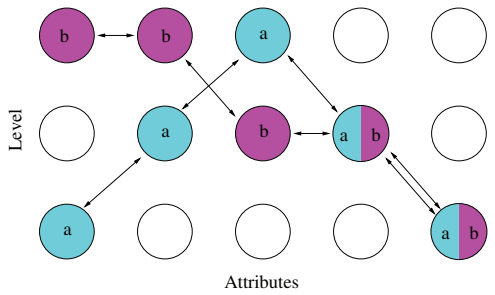

Figure 2. *A learned pattern is a set consisting of one cell from each attribute column and reciprocal excitatory connections between these cells. Two learned patterns are shown: pattern $A = (a_1, \ldots, a_5)$ and pattern $B = (b_1, \ldots, b_5)$. Cells in a learned pattern are all-to-all connected, though not all connections are indicated. Inhibitory connections are not indicated.*

and therefore has reciprocal excitatory connections corresponding to each of these patterns. In Figure 2 we illustrate a network with two learned patterns. We call cells that receive reciprocal excitatory connections *active*, and we call the other cells *inactive*.

Wilson (2009) assumes that there is a two-dimensional firing rate model identified with each network node. Hence there is a coupled system of $2mn$ differential equations associated to the rivalry network. Many authors have discussed the dynamics of firing rate models for rivalry. See Laing and Chow (2002), Moldakrimov et al. (2005), Seely and Chow (2011), Wilson (2003), Wilson (2007), Wilson (2009), Shpiro et al. (2007), Curtu et al. (2008), Curtu (2010), and Kilpatrick and Bressloff (2010). In this paper we present a method for reducing the high-dimensional models of Wilson (2009) to low-dimensional models, such as those studied by Curtu and coauthors.

We begin by listing our main contributions; then we discuss the background needed to understand them.

1. We identify regions in parameter and state space where the model of Wilson (2009) for two learned patterns can be rigorously reduced to either a well-studied two-node model (consisting of four equations) or a less well studied three-node model (consisting of six equations). Conversely, we show that the reduced models are embedded in Wilson's model, though we cannot prove that solutions that are stable in the reduced models

are stable in Wilson's model for all parameter values. Finally, we note that many regions of state space for Wilson's generalized models remain unexplored.

2. The two-node model is identical in form to the model of binocular rivalry considered by Curtu et al. (2008), with the exception that recurrent excitation is nonzero. Here, reciprocal excitation in the generalized model leads unavoidably to recurrent excitation in the reduced model.
3. The two-node model is known to exhibit many interesting dynamic states (including fusion, winner-take-all, rivalry, and mixed-mode oscillations) and transitions between these states. See Curtu (2010) for an extensive discussion. We show that some of what is known can be organized by tracking a degenerate path through the parameter space of a symmetry-breaking Takens–Bogdanov (TB) bifurcation.
   (a) The existence of TB points in the two-cell model (and its unfolding) implies the coexistence of a stable rivalry state and a stable winner-take-all state, which has not been mentioned previously in the literature with respect to the binocular rivalry model. See Shpiro et al. (2007) for a discussion of such bistability in a central pattern generator model originally considered by Taylor, Cottrell, and Kristan (2002).
   (b) The fact that the bifurcation parameter can vary degenerately through the TB point leads to different bifurcation diagrams. See Figures 9 and 10. Note that the diagram corresponding to path 3 seems not to have been observed previously.
4. We show that TB bifurcations also occur in the three-cell model. Hence, we learn much about the dynamics of this three-cell model just from having organized the results of the two-cell model around TB points.
5. Our methods make feasible the analysis of models based on three or more learned patterns, though this will be the subject of future work.
6. Although our specific analysis is based on a particular class of rate models studied by Wilson and others, our methods can be applied to a much larger class of equations.

1.1. Biological motivation for the generalized rivalry model. Binocular rivalry, the alternations in perception that occur when different images are presented to the two eyes, has frequently been touted as a powerful tool for studying neural correlates of conscious visual awareness (Blake and Logothetis (2002); Tong, Meng, and Blake (2006)). While most stimuli used in perceptual rivalry research allow exactly two distinct percepts, stimuli with more than two interpretations have been studied before (Burton (2002); Naber, Gruenhage, and Einhäuser (2010)). Wilson (2012) argues that generalizations of rivalry to multiple, partially overlapping patterns can provide key insights into aspects of conscious deliberation and decision making in the face of ambiguous or incomplete data.

The Wilson (2009) network model of interaction among multiple neural groups can be placed within the context of the anatomy of the brain areas critical for conscious vision. For example, suppose the network is involved with face recognition in the inferior temporal cortex. Here, the attribute columns might represent facial features such as eye separation or nose length. The rows within each column could then represent above average, average, or below average values for each feature. See page 406 of Wilson (2009) for further discussion and an alternative interpretation placing the network in the prefrontal cortex.

The Wilson (2009) model belongs to a class of competition models that incorporate neural adaptation, where activity associated to the currently dominant stimulus (or pattern) wanes over time (Blake and Wilson (2011)). Since the Wilson (2009) model is deterministic, it does not capture the noisy or irregular character of the perceptual alternations reported in rivalry experiments (van Ee (2009); Moreno-Bote, Rinzel, and Rubin (2007)). In order to reproduce all the dynamical behaviors exhibited during rivalry, neural models likely need to incorporate both adaptation and noise processes (Shpiro et al. (2009); Blake and Wilson (2011)). In this paper we do not incorporate noise and thus in effect are considering the mean switching behavior between perceptions.

We emphasize that our work is about the mathematical analysis of classes of models that have been and are being studied in the rivalry literature; this work is not directly about the neuroscience consequences of our results. We now introduce the models.

1.2. Equations for the generalized rivalry model. We denote the state variables for cell ij in the rivalry array by $X_{ij} = (X_{ij}^E, X_{ij}^H)$, where X_{ij}^E is an *activity* variable representing the firing rate of the ij node and X_{ij}^H is an *adaptation* (or hyperpolarizing) variable that reduces activity on a long time scale. We assume that these variables are nonnegative. The equation for each cell has the form

$$\begin{aligned} \varepsilon \dot{X}_{ij}^E &= -X_{ij}^E + \mathcal{G}\left(I_{ij} + w \sum_{pq \to ij} X_{pq}^E - \beta \sum_{rj \Rightarrow ij} X_{rj}^E - g X_{ij}^H \right), \\ \dot{X}_{ij}^H &= X_{ij}^E - X_{ij}^H, \end{aligned} \tag{1.1}$$

where $\to$ denotes an excitatory connection and $\Rightarrow$ denotes an inhibitory connection. Specifically, β denotes the strength of the *reciprocal inhibition* between cells in the same column, and w is the strength of the *reciprocal excitation* between cells in the same learned pattern. The function $\mathcal{G}$ is the *gain* and is usually assumed to be nonnegative and nondecreasing (see Laing and Chow (2001)). In this model, the adaptation variable X_{ij}^H reduces the activity variable X_{ij}^E with strength g and evolves on a longer time scale than the activity variables. Hence, ε is commonly, though not always, taken to be small. Note that the domain Ω defined by $X_{ij}^E \geq 0$ and $X_{ij}^H \geq 0$ is flow invariant for (1.1) since the gain function is nonnegative.

The inputs $I_{ij} \geq 0$ are external *signal strengths* to the patterns. We assume that the inputs I_{ij} satisfy the following:

(a) $I_{ij} = 0$ for every inactive cell ij.

(b) Each learned pattern P has an input $I_P \geq 0$. If ij is an active cell, then I_{ij} is the maximum of those I_P for which ij is an active cell in pattern P.

Later we assume that all of the I_P are positive and equal; that is, $I_P = I$ for all patterns P.

1.3. Gain functions and decay of inactive cells. We consider two types of gain functions in this paper: conforming and sigmoidal. Proposition 1.2 shows that if the gain function is conforming, then inactive cells decay to a base firing rate (0 in the models); thus inactive cells can be eliminated.

Definition 1.1. *Assume that the gain function $\mathcal{G}$ is smooth and satisfies the following:*

(a) $\mathcal{G}'(z) > 0$ *for* $z > \theta$.

(b) $\mathcal{G}'(z)$ *has a unique maximum at* $z = z_{max}$.

$\mathcal{G}$ *is* conforming *if, in addition, there exists a threshold* $\theta \geq 0$ *such that*

(c) $\mathcal{G}(z) = 0$ *for* $z \leq \theta$.

The gain is a sigmoid *if* (a) *and* (b) *are satisfied and*

(d) $\mathcal{G}(z) > 0$ *for all* z, $\lim_{z\to-\infty}\mathcal{G}(z) = 0$, *and* $\lim_{z\to+\infty}\mathcal{G}(z)$ *exists.*

Proposition 1.2. *Assume* $\mathcal{G}$ *is conforming. If cell* ij *is inactive, then* $X_{ij} = 0$ *is a flow-invariant subspace. Moreover, this subspace is globally attracting since* $X_{ij}(t) \to 0$ *as* $t \to \infty$.

Proof. Since cell ij is inactive, there are no excitatory connections to cell ij and $I_{ij} = 0$. Moreover, since $X^E_{rj} \geq 0$ and $X^H_{ij} \geq 0$,

$$z = -\beta\left(\sum_{rj\Rightarrow ij} X^E_{rj}\right) - gX^H_{ij} \leq 0 \leq \theta.$$

It follows from Definition 1.1(c) that $\mathcal{G}(z) = 0$, which implies

$$\varepsilon\dot{X}^E_{ij} = -X^E_{ij} + \mathcal{G}(z) = -X^E_{ij}.$$

Therefore, $\dot{X}_{ij} = 0$ when $X_{ij} = 0$ so that the subspace is flow-invariant, $X^E_{ij} \to 0$ exponentially, and X^H_{ij} follows. ∎

Remark 1.3. Proposition 1.2 leads to the $2n - k$ active node network shown in Figure 3 (left). The thresholded gain functions used by Wilson are conforming except for one point θ where a discontinuity in the first derivative occurs. As long as $\theta > 0$, Proposition 1.2 is still valid. ∎

Remark 1.4. Sigmoid functions are smooth, satisfy Definition 1.1(a) and (b), and approximately satisfy (d) since $\mathcal{G}(0)$ is usually very small. Under this assumption, we believe that the elimination of inactive cells based on conforming gain functions will be approximately true for sigmoidal gain functions. ∎

1.4. Quotient networks: Rivalry between two patterns. We make a second observation that simplifies the dynamics of the Wilson network: in certain parameter regimes active cells in a given row that belong to exactly one pattern synchronize, as do cells common to both patterns. In terms of the network in Figure 2, this observation implies that cells a_1, a_2, a_3 synchronize, as do cells b_1, b_2, b_3 and cells $a_4/b_4, a_5/b_5$. In fact, for all parameters, setting these three subsets of cells equal leads to a flow-invariant (polydiagonal) subspace for the dynamics. Hence, we may identify cells a_1, a_2, a_3 as a single cell and label the identified cell by a. Similarly, we may identify cells b_1, b_2, b_3 and label them by b and identify cells $a_4/b_4, a_5/b_5$ and label them by c. The network resulting from this identification is an example of a *quotient network* (Golubitsky, Stewart, and Török (2005); Golubitsky and Stewart (2006)). The fact that solutions with synchronized cells exist follows from quotient network theory; whether these synchronized states are stable depends on the specifics of the model equations.

There are two types of quotient networks that can be derived from the Wilson network for two learned patterns with inactive cells deleted: a two-cell quotient occurs when the two patterns have no cells in common, and a three-cell quotient occurs when the two patterns have active cells in common. Let k be the number of active cells in common between the two

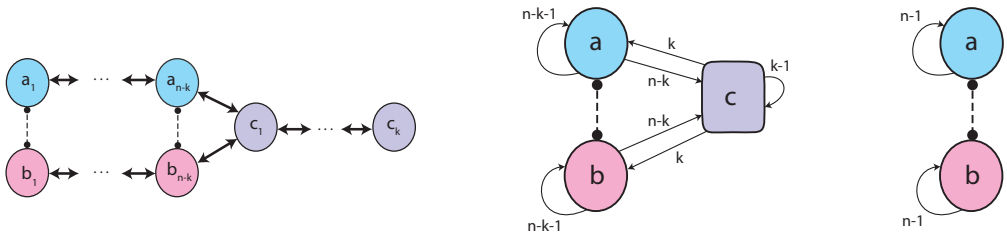

Figure 3. *Left: network with n attributes and two learned patterns with k cells in common. Cells within a pattern are all-to-all connected, though not all connections are indicated. Center: corresponding quotient network obtained by identifying cells with the same color when $k > 0$. Right: corresponding quotient network obtained by identifying cells with the same color when $k = 0$.*

patterns, as depicted in Figure 3 (left) (note that $k = 2$ in the network in Figure 2.) The three-cell quotient network ($k > 0$) is shown in Figure 3 (center), and the two-cell quotient network ($k = 0$) in Figure 3 (right).

The equations governing the two-cell quotient are identical to the equations for the simplest rivalry model with recurrent excitation (cf. Shpiro et al. (2007) and Wilson (2009)):

$$\begin{array}{rcl} \varepsilon\,\dot{a}^E &=& -a^E + \mathcal{G}\left(I + (n-1)wa^E - \beta b^E - ga^H\right), \\ \dot{a}^H &=& a^E - a^H, \\ \varepsilon\,\dot{b}^E &=& -b^E + \mathcal{G}\left(I + (n-1)wb^E - \beta a^E - gb^H\right), \\ \dot{b}_H &=& b^E - b^H, \end{array} \tag{1.2}$$

where $\alpha_0 = (n-1)w$ is the *effective* recurrent excitation. As noted previously, we will concentrate on the case $I_a = I_b = I$, where (1.2) has the transposition symmetry

$$\tau(a^E, a^H, b^E, b^H) = (b^E, b^H, a^E, a^H). \tag{1.3}$$

The model equations for the three-cell quotient network of Figure 3 when the two patterns have k active cells in common are

$$\begin{array}{rcl} \varepsilon\dot{a^E} &=& -a^E + \mathcal{G}(I + wkc^E + w(n-k-1)a^E - \beta b^E - ga^H), \\ \dot{a}^H &=& -a^H + a^E, \\ \varepsilon\dot{b^E} &=& -b^E + \mathcal{G}(I + wkc^E + w(n-k-1)b^E - \beta a^E - gb^H), \\ \dot{b}^H &=& -b^H + b^E, \\ \varepsilon\dot{c^E} &=& -c^E + \mathcal{G}(I + w(k-1)c^E + w(n-k)(a^E + b^E) - gc^H), \\ \dot{c}^H &=& -c^H + c^E, \end{array} \tag{1.4}$$

where I is the common input. Observe that cell c has $k-1$ self-excitatory connections from the other cells common to the two patterns; $n-k$ reciprocal excitatory connections from the cells not in common in patterns 1 and 2; and no inhibitory connections, since there is no other active cell in its column. We reiterate that the a, b cells in the quotient network have effective recurrent excitation

$$\alpha_k = w(n-1-k) \tag{1.5}$$

even though the corresponding cells in the original network had no recurrent excitation. Note that when $k = 0$ we recover α_0 from (1.5). The effective recurrent excitation in the c cells is $(k-1)w$. Observe that (1.4) has the nontrivial transposition symmetry

$$\tau(a^E, a^H, b^E, b^H, c^E, c^H) = (b^E, b^H, a^E, a^H, c^E, c^H). \tag{1.6}$$

Rivalry, winner-take-all, and fusion. In the binocular rivalry literature three types of states are described: rivalry, winner-take-all, and fusion. With respect to models these terms have the following interpretations:

- *rivalry* refers to oscillations in which two or more patterns alternate in dominance,
- *winner-take-all* (*WTA*) refers to a state in which the patterns are in equilibrium with one pattern at a higher activity level than the others, and
- *fusion* refers to an equilibrium in which patterns have equal values.

In the language of coupled cell theory, these states are represented by oscillations, asynchronous equilibria, and synchronous equilibria, respectively.

1.5. Takens–Bogdanov bifurcations as organizing centers. Systems (1.2) and (1.4) have five parameters (namely, w, g, ε, β, and I) and an unspecified function $\mathcal{G}$. It is difficult to determine all of the dynamics that might be present in these systems for different parameter values. From a dynamical systems perspective there are two ways to proceed. First, one can simulate the systems for a series of parameter values and a choice of gain function and then use numerical continuation to organize transitions in model behavior. Second, one can find degenerate singularities at special parameter values and understand (part of) the global dynamics by analyzing the unfolding of that degenerate singularity. Such singularities are called *organizing centers*.

Shpiro et al. (2007) and Curtu et al. (2008) take the first approach. They show in a variety of models, including the two-cell model (1.2) with $\alpha_0 = 0$, that fusion states transition to rivalry to WTA and back again as the input I is increased. See Figure 3 in Curtu (2010). We find similar results in the three-cell model (1.4). Figure 4 (left) shows the existence of states as a function of I; Figure 4 (right) shows simulations at particular values of I. Note that there is a Hopf bifurcation on the synchronous branch, followed by a pitchfork bifurcation. Then there is a Hopf bifurcation on the asynchronous branch. The branch of oscillations starts at the Hopf bifurcation on the synchronous branch and ends at the Hopf bifurcation on the asynchronous branch. As I continues to increase, this sequence is reversed.

In this paper we take the second approach. Based on simulation results (such as those in Figure 4), we conjectured a symmetry-breaking TB bifurcation as an organizing center.

Two observations led to this conjecture. First, the symmetry τ is important. This can be seen in the two-cell simulations where the two units oscillate a half-period out of phase. Such periodic solutions can result from symmetry-breaking Hopf bifurcation. In the three-cell system (1.4) the analogous bifurcation leads to periodic solutions where units a and b oscillate a half-period out of phase and cell c oscillates at twice the frequency. These periodic solutions have also been observed in simulations; see Figure 4 (right).

Second, the fact that on variation of I a symmetry-breaking Hopf bifurcation is followed by a pitchfork bifurcation in Figure 4 (left) suggests that the dynamics can be (partially) organized by a singularity in which these two bifurcations coalesce. Such a singularity occurs

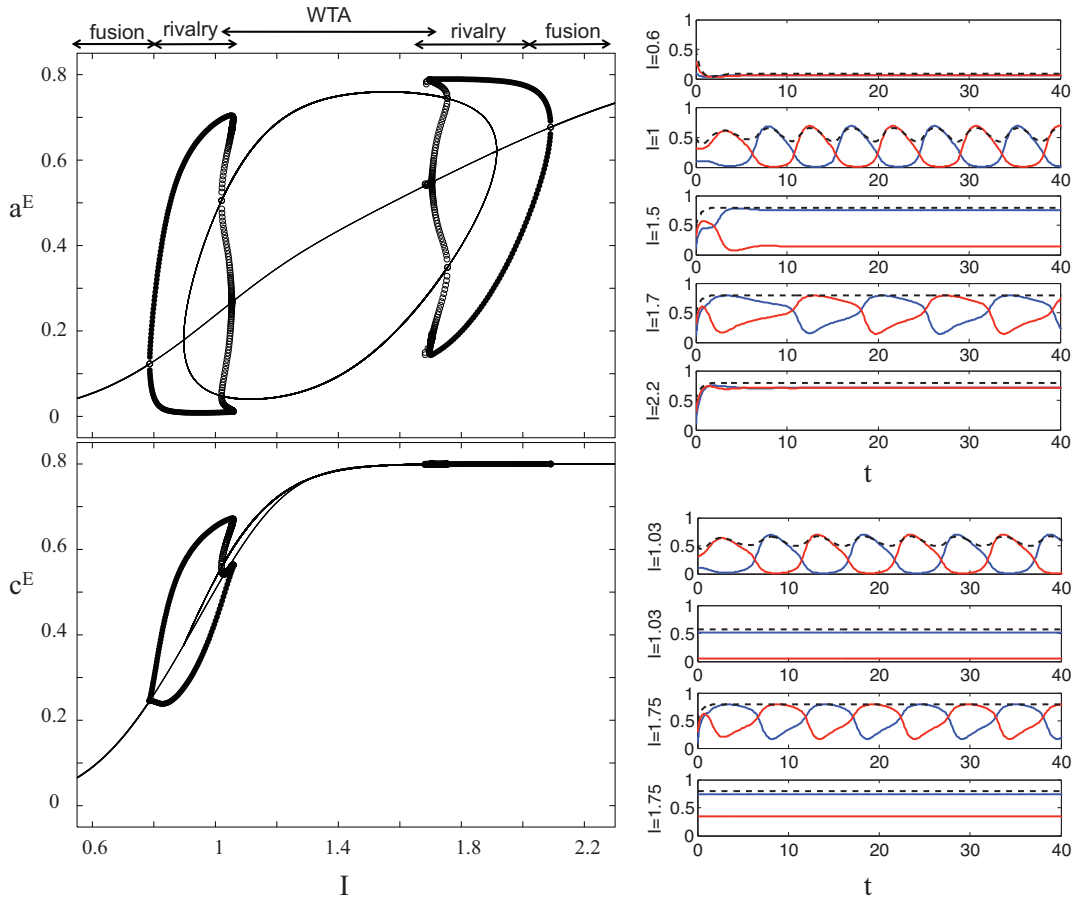

Figure 4. *Left: activity values a^E (upper) and c^E (lower) as a function of I for system (1.4) with the sigmoidal gain (4.9). Curves show steady states, and circles show the bounds of periodic orbits. Upper right: simulations in five regions noted at top left; time series show in order fusion, rivalry, WTA, rivalry, and fusion. Activity a^E is shown in blue, b^E in red, and c^E in black. Lower right: multiplicity of stable solutions (between rivalry and WTA) shown at $I = 1.03$ and $I = 1.75$. Here $w = 0.25$, $n = 5$, $k = 2$, $\beta = 1.5$, $g = 1$, $\varepsilon = 0.5$. These parameter values were identified by first finding a TB bifurcation in the three-cell reduction.*

when there is a double zero eigenvalue in the Jacobian at a synchronous equilibrium; that singularity type is known as the TB bifurcation (see Guckenheimer and Holmes (1983)). This TB bifurcation is not the standard one because of the τ symmetry in (1.6), but it is also studied in Guckenheimer and Holmes (1983).

We show that a symmetry-breaking TB bifurcation is present in both the two- and three-cell models (1.2) and (1.4) (see Propositions 3.4 and 3.5) and that various types of behavior, such as WTA, rivalry, and fusion, are present in the unfolding of this bifurcation (see Figure 5). Moreover, we show that in these models this bifurcation always occurs from a stable fusion state (see Theorem 3.7).

1.6. Organization of paper. In section 2 we use group representation theory to give a necessary and sufficient condition (2.1) that guarantees that for all ε solutions that are stable

in the two-cell and three-cell reductions of two-pattern networks are also stable in Wilson's model. See Theorem 2.2. Therefore, under these conditions, we can reduce the study of the original $2mn$-dimensional two-learned-pattern rivalry system to a four- or six-dimensional system, depending on whether the two patterns have active cells in common. The results in this section also enable us to prove in Theorem 3.7 that the dynamic reduction to the small networks is valid in a neighborhood of TB points whether or not (2.1) holds.

In section 3 we show how the symmetry-breaking TB singularity arises at certain critical parameter values; hence for parameter values near the critical ones we can further reduce the four- or six-dimensional system to a planar system. See Propositions 3.4 and 3.5. Consequently, we can infer the existence of parameter regions with competition between stable WTA equilibria and stable rivalry oscillations. See Figure 6.

In section 4 we discuss a degeneracy associated to having the input I as a distinguished bifurcation parameter. We show that implications that follow from the existence of this degeneracy can be verified numerically for sigmoidal gain functions. We observe that even though the TB singularity, its universal unfolding, and its degenerate distinguished parameter I have only local implications in parameter space, these implications seem to be valid over a large range of parameter space, at least in numerical explorations.

In section 5 we explore how parameter variation, particularly the amount of recurrent excitation, alters the qualitative behavior of solutions in the full system. We show that when the two patterns have no cells in common, increasing the amount of recurrent excitation causes the fusion state to lose stability at lower values of the input signal strength I (see Proposition 5.1) and can affect whether the transition is to rivalry or WTA (see Remark 5.4). On the other hand, increasing the number of cells in common between the two patterns increases the value of I where the fusion state loses stability (see Proposition 5.3).

The paper ends in section 6 with comments on future directions. We briefly discuss the quotient networks that can arise in reduction of the generalized rivalry model with three learned patterns, and we discuss generalized rivalry systems with many learned patterns.

2. Stability of synchrony subspaces.

Assuming that the gain function is conforming, Proposition 1.2 proves that cells that are inactive in all learned patterns stay quiet over time; that is, they converge to a base activity level of 0. It follows that the system can be reduced to a network consisting of those cells that are active in at least one learned pattern. See Figure 3 (left). In this section we assume that the reduction to the network of active cells has been performed, and we weaken the definition of gain function to be either conforming or sigmoidal.

The network in Figure 3 (left) has a number of symmetries. Indeed, every column permutation that preserves the common cells (and hence the cells that are not in common) is a symmetry of the network. That symmetry group is

$$\Sigma = \mathbf{S}_{n-k} \times \mathbf{S}_k.$$

The fixed-point subspace of Σ is the subspace obtained by setting the noncommon cells A in pattern 1 equal, the noncommon cells B in pattern 2 equal, and the common cells C equal. We denote

$$\mathcal{S} = \mathrm{Fix}(\Sigma).$$

It follows from general theory that $\mathcal{S}$ is flow-invariant and that the restriction of the dynamics to $\mathcal{S}$ is an admissible system of the three-cell quotient network in Figure 3 (right). See Golubitsky, Stewart, and Török (2005). Let F be an admissible system for the active cells network. Then flow-invariance just means that $F : \mathcal{S} \to \mathcal{S}$.

Let $X \in \mathcal{S}$, and let $(dF)_X$ be the Jacobian of F at X. It follows from Lemma 2.4 and Σ-equivariance that $(dF)_X$ leaves the orthogonal complement $\mathcal{S}^\perp$ invariant.

Definition 2.1. *The vector field F is* locally attracting *at $X \in \mathcal{S}$ if all eigenvalues of $(dF)_X|\mathcal{S}^\perp$ have negative real part. If F is locally attracting at every point in $X \in \mathcal{S}$, then F is* locally attracting globally *on $\mathcal{S}$.*

Theorem 2.2 gives conditions on F that show when the space $\mathcal{S}$ is locally attracting globally on $\mathcal{S}$, so that much of the dynamics of the mn-cell attribute network can be understood by analyzing the quotient dynamics on the appropriate two-cell or three-cell network. Theorem 3.7 uses these results to show that the subspace $\mathcal{S}$ is locally attracting near every symmetry-breaking TB bifurcation point. That is, near every TB point we can reduce the study of a system of $2mn$ equations to the study of the two normal form equations associated to the unfolding of this symmetry-breaking bifurcation.

2.1. Local attraction globally on $\mathcal{S}$. Numerical exploration seems to imply that $\mathcal{S}$ is locally attracting globally on $\mathcal{S}$. We have found a necessary and sufficient condition that validates this observation.

Theorem 2.2. *Suppose the gain function $\mathcal{G}$ is smooth and nondecreasing and has a unique point z_{max}, where $\mathcal{G}''(z_{max}) = 0$.*

(a) *If $\mathcal{S}$ is locally attracting globally on $\mathcal{S}$ for all small ε, then*

$$\beta < \frac{1}{\mathcal{G}'(z_{max})} + w. \tag{2.1}$$

(b) *If (2.1) is valid, then $\mathcal{S}$ is locally attracting globally on $\mathcal{S}$ for all ε.*

Remark 2.3. (a) Even if (2.1) fails, $\mathcal{S}$ can still be locally attracting along individual trajectories. In Theorem 3.7 we show this comment is valid for all bounded trajectories in the unfolding of a TB singularity.

(b) If, as Wilson (2009) assumes, the inhibition β is stronger than the excitation w, then (2.1) states that for local attraction globally on $\mathcal{S}$, the degree to which β can exceed w is bounded by the slope of the gain function $\mathcal{G}$. ■

The proof requires use of the symmetries Σ and a number of calculations. In particular, in order to prove Theorem 2.2 we use irreducible representations and isotypic components of Σ (Lemma 2.4), decompositions of the Jacobian based on these results (Proposition 2.8), and explicit calculations based on the exact form of the differential equations to compute the signs of eigenvalues (Lemmas 2.9–2.11). The proof of Theorem 2.2 is given in subsection 2.5.

2.2. Irreducible representations and isotypic components. In the next subsection we show that symmetry simplifies the computation of eigenvalues of Jacobian matrices through the use of irreducible representations and isotypic components. In this subsection we introduce these concepts and apply them to the two-pattern networks. Our reference is the second chapter of Golubitsky, Stewart, and Schaeffer (1988).

An action of a finite group Σ on $\mathbb{R}^n$ can always be decomposed into a direct sum of irreducible representations; that is,

$$\mathbb{R}^n = W_1 \oplus \cdots \oplus W_k, \tag{2.2}$$

where Σ acts irreducibly on each W_j. This decomposition need not be unique; nonuniqueness stems from the occurrence of isomorphic irreducible representations in (2.2).

However, uniqueness can be recovered by considering isotypic components. Given an irreducible representation W, we can form the *isotypic component* V of W, which is the sum of all irreducible representations in $\mathbb{R}^n$ that are isomorphic to W. Renumber so that $W_1, \ldots, W_\ell$ lists the distinct irreducible representations ($\ell \leq k$) of Σ acting on $\mathbb{R}^n$, and let $V_1, \ldots, V_\ell$ be the associated isotypic components. Theory shows that

$$\mathbb{R}^n = V_1 \oplus \cdots \oplus V_\ell \tag{2.3}$$

and this decomposition is unique.

We denote the active cells by X and partition the active cells into three groups: A (active cells in pattern A), B (active cells in pattern B), and C (common active cells), where

$$\begin{array}{rcl} A & = & (X_{11}, \ldots, X_{1,n-k}), \\ B & = & (X_{21}, \ldots, X_{2,n-k}), \\ C & = & (X_{1,n-k+1}, \ldots, X_{1,n}). \end{array}$$

To reduce the notational complexity we set $a_i = X_{1i}$, $b_i = X_{2i}$, and $c_i = X_{1,n-k+i}$ so that $A = (a_1, \ldots, a_{n-k})$, $B = (b_1, \ldots, b_{n-k})$, and $C = (c_1, \ldots, c_k)$.

The subgroup $\mathbf{S}_{n-k}$ acts on X by simultaneously permuting the a_j and b_j and fixing c. The subgroup $\mathbf{S}_k$ acts on X by permuting the c_i and fixing a and b. It follows that

$$\mathcal{S} = \mathrm{Fix}(\Sigma) = \{(a, \ldots, a, b, \ldots, b, c, \ldots, c) : a, b, c \in \mathbb{R}^2\}.$$

Note that $\mathrm{Fix}(\Sigma)$ is six-dimensional and that the subgroup Σ acts trivially on $\mathrm{Fix}(\Sigma)$.

We next write the orthogonal complement of $\mathrm{Fix}(\Sigma)$ as a direct sum of irreducible representations. Define

$$\begin{array}{rcl} W_A^E & = & \{((A^E, 0), 0, 0) : a_1^E + \cdots + a_{n-k}^E = 0\}, \\ W_A^H & = & \{((0, A^H), 0, 0) : a_1^H + \cdots + a_{n-k}^H = 0\}, \\ W_A & = & W_A^E \oplus W_A^H = \{(A, 0, 0) : a_1 + \cdots + a_{n-k} = 0\}, \end{array}$$

and similarly for B and C.

Lemma 2.4. *The action of Σ on each subspace $W_A^E, W_A^H, W_B^E, W_B^H, W_C^E, W_C^H$ is irreducible, and*

$$\mathrm{Fix}(\Sigma)^\perp = W_A^E \oplus W_A^H \oplus W_B^E \oplus W_B^H \oplus W_C^E \oplus W_C^H.$$

The isotypic decomposition of the phase space of the two-pattern network is

$$\mathbb{R}^{2n} = \mathrm{Fix}(\Sigma) \oplus V_1 \oplus V_2,$$

where $V_1 = W_A \oplus W_B$ and $V_2 = W_C$.

Proof. The actions of Σ on W_C^E and W_C^H are isomorphic, and similarly for the A and B subspaces. The action of Σ on W_A^E and W_B^E are also isomorphic. Finally, the actions of Σ on W_A^E and W_C^E are not isomorphic (they have different kernels). ∎

The synchronous symmetry. When the inputs are equal, the network system has an extra $\mathbf{Z}_2$ symmetry τ defined in (1.6). The actions of Σ and τ commute; hence there is an action of $\Sigma \oplus \mathbf{Z}_2(\tau)$ on the (A, B, C) phase space. Note that $\mathbf{Z}_2$ acts trivially on W_C and leaves $W_A \oplus W_B$ invariant. Let

$$V_+ = \{(A, A, 0) : a_1 + \cdots + a_{n-k} = 0\}, \qquad V_- = \{(A, -A, 0) : a_1 + \cdots + a_{n-k} = 0\},$$

and note that τ acts trivially on V_+ and as $-\mathrm{Id}$ on V_-. This discussion proves the following lemma.

Lemma 2.5. *The isotypic decomposition of* $\mathrm{Fix}(\Sigma \oplus \mathbf{Z}_2)^\perp$ *is*

$$\mathrm{Fix}(\Sigma \oplus \mathbf{Z}_2)^\perp = V_+ \oplus V_- \oplus V_2.$$

2.3. Commuting linear maps. Suppose that $\sigma \in \Sigma$ is a symmetry of the differential equation $\dot{X} = F(X)$, that is, $F(\sigma X) = \sigma F(X)$, and that $\sigma X_0 = X_0$. The chain rule implies that

$$\sigma (DF)_{X_0} = (DF)_{X_0} \sigma.$$

It follows that the Jacobian matrix $J = (DF)_{X_0}$ commutes with Σ for any point $X_0 \in \mathrm{Fix}(\Sigma)$. The basic theorem about commuting linear maps J and isotypic components V states that

$$J(V) \subset V.$$

Hence, J is block diagonal with respect to the isotypic decomposition (2.3).

In fact, symmetry can further specify J. Suppose that the isotypic component is written as

$$V = U_1 \oplus \cdots \oplus U_m,$$

where the U_j are isomorphic irreducible representations. Then the linear map $J|V$ has the block form

$$J|V = \begin{pmatrix} J_{11} & \cdots & J_{1m} \\ \vdots & \vdots & \vdots \\ J_{m1} & \cdots & J_{mm} \end{pmatrix}, \tag{2.4}$$

where $J_{ij} : U_j \to U_i$ commutes with the action of Σ on the U_j.

Next, we recall that real irreducible representations U come in two types: *absolutely irreducible* and *nonabsolutely irreducible*. The absolutely irreducible representations are the ones for which every commuting linear map is a scalar multiple of the identity.

Example 2.6. Suppose the permutation group $\mathbf{S}_\ell$ acts on $\mathbb{R}^\ell$ by permuting coordinates. It is well known that the space

$$U = \{(y_1, \ldots, y_\ell) \in \mathbb{R}^\ell : y_1 + \cdots + y_\ell = 0\}$$

is an absolutely irreducible representation of $\mathbf{S}_\ell$. ■

If the representation of Σ on U is absolutely irreducible and $\dim U = p$, then

$$J|V = \begin{pmatrix} \chi_{11} I_p & \cdots & \chi_{1m} I_p \\ \vdots & \vdots & \vdots \\ \chi_{m1} I_p & \cdots & \chi_{mm} I_p \end{pmatrix}, \tag{2.5}$$

where $\chi_{ij} \in \mathbb{R}$. Note that the eigenvalues of the matrix of $J|V$ given in (2.5) are just the eigenvalues of the $m \times m$ matrix

$$\chi = \begin{pmatrix} \chi_{11} & \cdots & \chi_{1m} \\ \vdots & \vdots & \vdots \\ \chi_{m1} & \cdots & \chi_{mm} \end{pmatrix} \tag{2.6}$$

each repeated p times, a huge reduction.

Suppose we write the vector field as $\dot{X} = \mathcal{F}(X)$ and the Jacobian matrix as $J_X = (D\mathcal{F})_X$. The theory just outlined implies that $J_X : V_1 \to V_1$ and $J_X : V_2 \to V_2$, and we denote

$$J_X^1 = J_X|V_1 \quad \text{and} \quad J_X^2 = J_X|V_2.$$

Next we use the fact that the irreducible representations of Σ are absolutely irreducible. Thus

$$J_X^1 \equiv J_X|(W_A^E \oplus W_A^H \oplus W_B^E \oplus W_B^H) = \begin{pmatrix} \zeta_{11}I_{n-k-1} & \zeta_{12}I_{n-k-1} & \zeta_{13}I_{n-k-1} & \zeta_{14}I_{n-k-1} \\ \zeta_{21}I_{n-k-1} & \zeta_{22}I_{n-k-1} & \zeta_{23}I_{n-k-1} & \zeta_{24}I_{n-k-1} \\ \zeta_{31}I_{n-k-1} & \zeta_{32}I_{n-k-1} & \zeta_{33}I_{n-k-1} & \zeta_{34}I_{n-k-1} \\ \zeta_{41}I_{n-k-1} & \zeta_{42}I_{n-k-1} & \zeta_{43}I_{n-k-1} & \zeta_{44}I_{n-k-1} \end{pmatrix}. \tag{2.7}$$

Similarly,

$$J_X^2 \equiv J_X|(W_C^E \oplus W_C^H) = \begin{pmatrix} \xi_{11}I_{k-1} & \xi_{12}I_{k-1} \\ \xi_{21}I_{k-1} & \xi_{22}I_{k-1} \end{pmatrix}. \tag{2.8}$$

Lemma 2.7. *Let $X \in \mathrm{Fix}(\Sigma)$. The eigenvalues of the Jacobian matrix J_X restricted to $\mathrm{Fix}(\Sigma)^\perp$ are given by the eigenvalues of the 2×2 matrix*

$$\xi = \begin{pmatrix} \xi_{11} & \xi_{12} \\ \xi_{21} & \xi_{22} \end{pmatrix}$$

repeated $k-1$ times and by the eigenvalues of the 4×4 matrix

$$\zeta = \begin{pmatrix} \zeta_{11} & \zeta_{12} & \zeta_{13} & \zeta_{14} \\ \zeta_{21} & \zeta_{22} & \zeta_{23} & \zeta_{24} \\ \zeta_{31} & \zeta_{32} & \zeta_{33} & \zeta_{34} \\ \zeta_{41} & \zeta_{42} & \zeta_{43} & \zeta_{44} \end{pmatrix}$$

repeated $n-k-1$ times.

Proof. The proof follows from (2.7) and (2.8) in the way that (2.6) follows from (2.5). ∎

Recall that a point $X \in \mathcal{S}$ is *synchronous* if $\tau X = X$. More precisely, $\tau(A,B,C) = (B,A,C)$, so X is synchronous if $A = B$. At such points the computation of the eigenvalues of J_X further simplifies since J_X will commute with the matrix

$$\tau = \begin{pmatrix} 0 & I_{2(n-k)} & 0 \\ I_{2(n-k)} & 0 & 0 \\ 0 & 0 & I_{2k} \end{pmatrix}.$$

It follows that ζ has the form

$$\zeta = \begin{pmatrix} \phi & \psi \\ \psi & \phi \end{pmatrix}, \tag{2.9}$$

where ϕ, ψ are 2×2 matrices. The 2×2 matrices corresponding to $J_X|V_+$ and $J_X|V_-$ are $\phi \pm \psi$. Note that

$$\phi \pm \psi = \begin{pmatrix} \zeta_{11} \pm \zeta_{13} & \zeta_{12} \pm \zeta_{14} \\ \zeta_{21} \pm \zeta_{23} & \zeta_{22} \pm \zeta_{24} \end{pmatrix}.$$

Proposition 2.8. *Let $X \in \mathcal{S}$ be a synchronous point. Then $\mathcal{S}$ is locally attracting at X if and only if*

$$\begin{array}{rcl} \operatorname{tr}(\phi+\psi) < 0 & \text{and} & \det(\phi+\psi) > 0, \\ \operatorname{tr}(\phi-\psi) < 0 & \text{and} & \det(\phi-\psi) > 0, \\ \operatorname{tr}(\xi) < 0 & \text{and} & \det(\xi) > 0. \end{array}$$

Proof. The eigenvalues of a 2×2 matrix have negative real part if and only if the matrix has negative trace and positive determinant. ∎

2.4. Computation of ζ and ξ from $\mathcal{F}$. In this subsection we compute the matrices ξ and ζ (and hence ϕ and ψ) from $\mathcal{F}$. In cell-type coordinates the equations for the two-pattern network in Figure 3 (left) have the form

$$\mathcal{F}(A,B,C) = (\mathcal{A}(A,B,C), \mathcal{B}(A,B,C), \mathcal{C}(A,B,C)),$$

where $\mathcal{A} = (\mathcal{A}_1, \dots, \mathcal{A}_{n-k})$, $\mathcal{B} = (\mathcal{B}_1, \dots, \mathcal{B}_{n-k})$, and $\mathcal{C} = (\mathcal{C}_1, \dots, \mathcal{C}_k)$.

Lemma 2.9. *Suppose that $X \in \mathcal{S}$. Then the entries to the matrix ξ are*

$$\xi_{11} = \frac{\partial \mathcal{C}_1^E}{\partial c_1^E} - \frac{\partial \mathcal{C}_2^E}{\partial c_1^E}, \quad \xi_{21} = \frac{\partial \mathcal{C}_1^E}{\partial c_1^H} - \frac{\partial \mathcal{C}_2^E}{\partial c_1^H}, \quad \xi_{22} = \frac{\partial \mathcal{C}_1^H}{\partial c_1^H} - \frac{\partial \mathcal{C}_2^H}{\partial c_1^H}, \quad \xi_{12} = \frac{\partial \mathcal{C}_1^H}{\partial c_1^E} - \frac{\partial \mathcal{C}_2^H}{\partial c_1^E}.$$

Proof. In the cell coordinates the Jacobian is

$$D\mathcal{F} = \begin{pmatrix} D_A\mathcal{A} & D_A\mathcal{B} & D_A\mathcal{C} \\ D_B\mathcal{A} & D_B\mathcal{B} & D_B\mathcal{C} \\ D_C\mathcal{A} & D_C\mathcal{B} & D_C\mathcal{C} \end{pmatrix},$$

since W_A^E and W_B^E are isomorphic absolutely irreducible representations of Σ that are distinct from the absolutely irreducible representation W_C^E. The invariant subspace V_2 implies

$$J_X^2(V_2) = (D_C\mathcal{C})_X(V_2).$$

Order the c variables by $(C^E, C^H) = (c_1^E, \dots, c_k^E, c_1^H, \dots, c_k^H)^t$, and let

$$v_2 = (1, -1, 0, \dots, 0) \in \mathbb{R}^k \quad \text{and} \quad v_2^E = (v_2, 0)^t \in \mathbb{R}^{2k}.$$

Order the $\mathcal{C}$ coordinates of $\mathcal{F}$ by $\mathcal{C} = (\mathcal{C}^E, \mathcal{C}^H)$. Then

$$J_X^2 = \begin{pmatrix} (D_{C^E}\mathcal{C}^E)_X & (D_{C^E}\mathcal{C}^H)_X \\ (D_{C^H}\mathcal{C}^E)_X & (D_{B^H}\mathcal{C}^H)_X \end{pmatrix}.$$

Now compute

$$J_X^2 v_2^E = \begin{pmatrix} (D_{C^E}\mathcal{C}^E)_X v_2 \\ (D_{C^H}\mathcal{C}^E)_X v_2 \end{pmatrix} = \begin{pmatrix} \xi_{11} v_2 \\ \xi_{21} v_2 \end{pmatrix}. \tag{2.10}$$

By equating the first coordinate in (2.10) we find the first identity, and by equating the $(k+1)$st coordinate we verify the second identity. We do this similarly for the third and fourth identities. ∎

Lemma 2.10. *Suppose that $X \in \mathcal{S}$. Then the entries to the matrix ζ are*

$$\begin{aligned}
\zeta_{11} &= \frac{\partial \mathcal{A}_1^E}{\partial a_1^E} - \frac{\partial \mathcal{A}_2^E}{\partial a_1^E}, & \zeta_{12} &= \frac{\partial \mathcal{A}_1^H}{\partial a_1^E} - \frac{\partial \mathcal{A}_2^H}{\partial a_1^E}, & \zeta_{13} &= \frac{\partial \mathcal{B}_1^E}{\partial a_1^E} - \frac{\partial \mathcal{B}_2^E}{\partial a_1^E}, & \zeta_{14} &= \frac{\partial \mathcal{B}_1^H}{\partial a_1^E} - \frac{\partial \mathcal{B}_2^H}{\partial a_1^E}, \\
\zeta_{21} &= \frac{\partial \mathcal{A}_1^E}{\partial a_1^H} - \frac{\partial \mathcal{A}_2^E}{\partial a_1^H}, & \zeta_{22} &= \frac{\partial \mathcal{A}_1^H}{\partial a_1^H} - \frac{\partial \mathcal{A}_2^H}{\partial a_1^H}, & \zeta_{23} &= \frac{\partial \mathcal{B}_1^E}{\partial a_1^H} - \frac{\partial \mathcal{B}_2^E}{\partial a_1^H}, & \zeta_{24} &= \frac{\partial \mathcal{B}_1^H}{\partial a_1^H} - \frac{\partial \mathcal{B}_2^H}{\partial a_1^H}, \\
\zeta_{31} &= \frac{\partial \mathcal{A}_1^E}{\partial b_1^E} - \frac{\partial \mathcal{A}_2^E}{\partial b_1^E}, & \zeta_{32} &= \frac{\partial \mathcal{A}_1^H}{\partial b_1^E} - \frac{\partial \mathcal{A}_2^H}{\partial b_1^E}, & \zeta_{33} &= \frac{\partial \mathcal{B}_1^E}{\partial b_1^E} - \frac{\partial \mathcal{B}_2^E}{\partial b_1^E}, & \zeta_{34} &= \frac{\partial \mathcal{B}_1^H}{\partial b_1^E} - \frac{\partial \mathcal{B}_2^H}{\partial b_1^E}, \\
\zeta_{41} &= \frac{\partial \mathcal{A}_1^E}{\partial b_1^H} - \frac{\partial \mathcal{A}_2^E}{\partial b_1^H}, & \zeta_{42} &= \frac{\partial \mathcal{A}_1^H}{\partial b_1^H} - \frac{\partial \mathcal{A}_2^H}{\partial b_1^H}, & \zeta_{43} &= \frac{\partial \mathcal{B}_1^E}{\partial b_1^H} - \frac{\partial \mathcal{B}_2^E}{\partial b_1^H}, & \zeta_{44} &= \frac{\partial \mathcal{B}_1^H}{\partial b_1^H} - \frac{\partial \mathcal{B}_2^H}{\partial b_1^H}.
\end{aligned}$$

Proof. We compute ζ_{ij} in the same way as we did for ξ_{ij}. The invariant subspace V_1 implies

$$J_X^1(V_1) = \begin{pmatrix} (D_A\mathcal{A})_X & (D_A\mathcal{B})_X \\ (D_B\mathcal{A})_X & (D_B\mathcal{B})_X \end{pmatrix}(V_1).$$

Order the A, B variables by

$$(A, B) = (a_1^E, \dots, a_{n-k}^E, a_1^H, \dots, a_{n-k}^H, b_1^E, \dots, b_{n-k}^E, b_1^H, \dots, b_{n-k}^H,),$$

and order $\mathcal{A}, \mathcal{B}$ similarly. Note that

$$J_X^1 = \begin{pmatrix} (D_{A^E}\mathcal{A}^E)_X & (D_{A^E}\mathcal{A}^H)_X & (D_{A^E}\mathcal{B}^E)_X & (D_{A^E}\mathcal{B}^H)_X \\ (D_{A^H}\mathcal{A}^E)_X & (D_{A^H}\mathcal{A}^H)_X & (D_{A^H}\mathcal{B}^E)_X & (D_{A^H}\mathcal{B}^H)_X \\ (D_{B^E}\mathcal{A}^E)_X & (D_{B^E}\mathcal{A}^H)_X & (D_{B^E}\mathcal{B}^E)_X & (D_{B^E}\mathcal{B}^H)_X \\ (D_{B^H}\mathcal{A}^E)_X & (D_{B^H}\mathcal{A}^H)_X & (D_{B^H}\mathcal{B}^E)_X & (D_{B^H}\mathcal{B}^H)_X \end{pmatrix}.$$

Let $v_1 = (1, -1, 0, \dots, 0) \in \mathbb{R}^{n-k}$ and $v_1^E = (v_1, 0, 0, 0)^t \in \mathbb{R}^{4(n-k)}$. Then

$$J_X^1 v_1^E = \begin{pmatrix} (D_{A^E}\mathcal{A}^E)_X v_1 \\ (D_{A^H}\mathcal{A}^E)_X v_1 \\ (D_{B^E}\mathcal{A}^E)_X v_1 \\ (D_{B^H}\mathcal{A}^E)_X v_1 \end{pmatrix} = \begin{pmatrix} \zeta_{11} v_1 \\ \zeta_{21} v_1 \\ \zeta_{31} v_1 \\ \zeta_{41} v_1 \end{pmatrix}. \tag{2.11}$$

By equating coordinates in (2.11), we find $\zeta_{11}, \dots, \zeta_{4,1}$. A similar calculation yields ζ_{ij}. ∎

Explicit computation of ζ and ξ. Our next task is to calculate the entries of ζ and ξ from the actual differential equations of the network in Figure 3 (left).

Lemma 2.11. *Assume that $X \in \mathcal{S}$. Then the entries of ξ and ζ are*

$$\begin{array}{llllllll}
\xi_{11} = -\frac{1}{\varepsilon}(1+w\mathcal{G}'(z_c)), & \xi_{21} = \frac{1}{\varepsilon}\{-\mathcal{G}'(z_c)g\}, & \xi_{22} = -1, & \xi_{12} = 1, \\
\zeta_{11} = -\frac{1}{\varepsilon}(1+w\mathcal{G}'(z_a)), & \zeta_{12} = 1, & \zeta_{13} = -\frac{1}{\varepsilon}\beta\mathcal{G}'(z_b), & \zeta_{14} = 0, \\
\zeta_{21} = -\frac{1}{\varepsilon}g\mathcal{G}'(z_a), & \zeta_{22} = -1, & \zeta_{23} = 0, & \zeta_{24} = 0, \\
\zeta_{31} = -\frac{1}{\varepsilon}\beta\mathcal{G}'(z_a), & \zeta_{32} = 0, & \zeta_{33} = -\frac{1}{\varepsilon}(1+w\mathcal{G}'(z_b)), & \zeta_{34} = 1, \\
\zeta_{41} = 0, & \zeta_{42} = 0, & \zeta_{43} = -\frac{1}{\varepsilon}g\mathcal{G}'(z_b), & \zeta_{44} = -1,
\end{array}$$

where

$$\begin{aligned}
z_c &= I + w\left\{(n-k)(a^E+b^E)+(k-1)c^E\right\} - gc^H, \\
z_a &= I + w\left\{(n-k-1)a^E+kc^E\right\} - \beta b^E - ga^H, \\
z_b &= I + w\left\{(n-k-1)b^E+kc^E\right\} - \beta a^E - gb^H,
\end{aligned} \tag{2.12}$$

and a^E, a^H, b^E, b^H, c^E, c^H are the common values of a_i^E, a_i^H, $b_i^E, b_i^H, c_i^E, c_i^H$ for all i.

Proof. The differential equations of the network in Figure 3 (left) have the form

$$\begin{aligned}
\dot{a}_1 &= \mathcal{A}_1(a_1, \overline{a_2,\dots,a_{n-k}}, b_1, \overline{c_1,\dots,c_k}) \\
&\vdots \\
\dot{a}_{n-k} &= \mathcal{A}_{n-k}(a_{n-k}, \overline{a_1,\dots,a_{n-k-1}}, b_{n-k}, \overline{c_1,\dots,c_k}) \\
\dot{b}_1 &= \mathcal{B}_1(b_1, \overline{b_2,\dots,b_{n-k}}, a_1, \overline{c_1,\dots,c_k}) \\
&\vdots \\
\dot{b}_{n-k} &= \mathcal{B}_{n-k}(b_{n-k}, \overline{b_1,\dots,b_{n-k-1}}, a_{n-k}, \overline{c_1,\dots,c_k}) \\
\dot{c}_1 &= \mathcal{C}_1(c_1, \overline{c_2,\dots,c_k}, \overline{a_1,\dots,a_{n-k}}, \overline{b_1,\dots,b_{n-k}}) \\
&\vdots \\
\dot{c}_k &= \mathcal{C}_k(c_k, \overline{c_1,\dots,c_{k-1}}, \overline{a_1,\dots,a_{n-k}}, \overline{b_1,\dots,b_{n-k}}).
\end{aligned} \tag{2.13}$$

The overline indicates that the functions are independent of the ordering of the variables under the line. Specifically,

$$\begin{aligned}
&\mathcal{A}_1(a_1, \overline{a_2,\dots,a_{n-k}}, b_1, \overline{c_1,\dots,c_k}) \\
&\qquad = \begin{bmatrix} \frac{1}{\varepsilon}\left\{-a_1^E + \mathcal{G}\left(I + w\left\{\sum_{s=2}^{n-k} a_s^E + \sum_{s=1}^{k} c_s^E\right\} - \beta b_1^E - g a_1^H\right)\right\} \\ a_1^E - a_1^H \end{bmatrix},
\end{aligned}$$

$$\mathcal{B}_1(b_1, \overline{b_2, \ldots, b_{n-k}}, a_1, \overline{c_1, \ldots, c_k})$$
$$= \begin{bmatrix} \frac{1}{\varepsilon}\left\{-b_1^E + \mathcal{G}\left(I + w\left\{\sum_{s=2}^{n-k} b_s^E + \sum_{s=1}^{k} c_s^E\right\} - \beta a_1^E - g b_1^H)\right)\right\} \\ b_1^E - b_1^H \end{bmatrix},$$

$$\mathcal{C}_1(c_1, \overline{c_2, \ldots, c_k}, \overline{a_1, \ldots, a_{n-k}}, \overline{b_1, \ldots, b_{n-k}})$$
$$= \begin{bmatrix} \frac{1}{\varepsilon}\left\{-c_s^E + \mathcal{G}\left(I + w\left\{\sum_{s=1}^{n-k} (a_s^E + b_s^E) + \sum_{s=2}^{k} c_s^E\right\} - g c_1^H)\right)\right\} \\ c_1^E - c_1^H \end{bmatrix}.$$

We compute the attraction to $\mathcal{S}$ at a point $X = (a, \ldots, a, b, \ldots, b, c, \ldots, c) \in \mathcal{S}$. Hence

$$\mathcal{C}_1(c_1, \overline{c_2, \ldots, c_k}, \overline{a_1, \ldots, a_{n-k}}, \overline{b_1, \ldots, b_{n-k}}) = \begin{bmatrix} \frac{1}{\varepsilon}\left\{-c_1^E + \mathcal{G}(z_{c_1})\right\} \\ c_1^E - c_1^H \end{bmatrix},$$
$$\mathcal{C}_2(c_2, \overline{c_1, c_3, \ldots, c_k}, \overline{a_1, \ldots, a_{n-k}}, \overline{b_1, \ldots, b_{n-k}}) = \begin{bmatrix} \frac{1}{\varepsilon}\left\{-c_2^E + \mathcal{G}(z_{c_2})\right\} \\ c_2^E - c_2^H \end{bmatrix},$$
$$\mathcal{A}_1(a_1, \overline{a_2, \ldots, a_{n-k}}, b_1, \overline{c_1, \ldots, c_k}) = \begin{bmatrix} \frac{1}{\varepsilon}\left\{-a_1^E + \mathcal{G}(z_{a_1})\right\} \\ a_1^E - a_1^H \end{bmatrix},$$
$$\mathcal{A}_2(a_2, \overline{a_1, a_3, \ldots, a_{n-k}}, b_2, \overline{c_1, \ldots, c_k}) = \begin{bmatrix} \frac{1}{\varepsilon}\left\{-a_2^E + \mathcal{G}(z_{a_2})\right\} \\ a_2^E - a_2^H \end{bmatrix},$$
$$\mathcal{B}_1(b_1, \overline{b_2, \ldots, b_{n-k}}, a_1, \overline{c_1, \ldots, c_k}) = \begin{bmatrix} \frac{1}{\varepsilon}\left\{-b_1^E + \mathcal{G}(z_{b_1})\right\} \\ b_1^E - b_1^H \end{bmatrix},$$
$$\mathcal{B}_2(b_2, \overline{b_1, b_3, \ldots, b_{n-k}}, a_2, \overline{c_1, \ldots, c_k}) = \begin{bmatrix} \frac{1}{\varepsilon}\left\{-b_2^E + \mathcal{G}(z_{b_2})\right\} \\ b_2^E - b_2^H \end{bmatrix},$$

where

$$z_{c_1} = I + w\left\{\sum_{s=1}^{n-k} (a_s^E + b_s^E) + \sum_{s\neq i}^{k} c_s^E\right\} - g c_1^H,$$
$$z_{c_2} = I + w\left\{\sum_{s=1}^{n-k} (a_s^E + b_s^E) + \sum_{s\neq 2}^{k} c_s^E\right\} - g c_2^H,$$
$$z_{a_1} = I + w\left\{\sum_{s\neq 1}^{n-k} a_s^E + \sum_{s=n-k+1}^{n} c_s^E\right\} - \beta b_1^E - g a_1^H,$$
$$z_{a_2} = I + w\left\{\sum_{s\neq 2}^{n-k} a_s^E + \sum_{s=n-k+1}^{n} c_s^E\right\} - \beta b_2^E - g a_2^H,$$

$$z_{b_1} = I + w\left\{\sum_{s\neq 1}^{n-k} b_s^E + \sum_{s=n-k+1}^{n} c_s^E\right\} - \beta a_1^E - g b_1^H,$$

$$z_{b_2} = I + w\left\{\sum_{s\neq 2}^{n-k} b_s^E + \sum_{s=n-k+1}^{n} c_s^E\right\} - \beta a_2^E - g b_2^H.$$

Note that for points in $\mathcal{S}$, $z_{c_1} = z_{c_2} = z_c$, $z_{a_1} = z_{a_2} = z_a$, $z_{b_1} = z_{b_2} = z_b$. Otherwise, z_a, z_b, z_c are arbitrary points in $\mathbb{R}$. Lemmas 2.9 and 2.10 give the desired results for ξ_{ij} and ζ_{ij}. ■

Lemma 2.12. *For all $X \in \mathcal{S}$ the eigenvalues of the 2×2 matrix ξ have negative real part.*

Proof. It follows from Lemma 2.11 that

$$\operatorname{tr}(\xi) = \xi_{11} + \xi_{22} = -\frac{1}{\varepsilon}(1 + w\mathcal{G}'(z_c)) - 1$$

and

$$\det(\xi) = \xi_{11}\xi_{22} - \xi_{12}\xi_{21} = \frac{1}{\varepsilon}(1 + w\mathcal{G}'(z_c) + \mathcal{G}'(z_c)g).$$

Since $\mathcal{G}' \geq 0$, we have $\operatorname{tr}(\xi) < 0$ and $\det(\xi) > 0$. ■

2.5. Proof of Theorem 2.2. Lemma 2.7 states that $\operatorname{Fix}(\Sigma)$ is locally attracting only if the eigenvalues of ξ and ζ have negative real part. Lemma 2.12 states that at each point $X \in \mathcal{S}$, the eigenvalues of ξ have negative real part. So we need only show that ζ has eigenvalues with negative real part. By Lemma 2.11,

$$\zeta = \frac{1}{\varepsilon}\hat{\zeta} \equiv \frac{1}{\varepsilon}\begin{pmatrix} -(1+w\mathcal{G}'(z_a)) & \varepsilon & -\beta\mathcal{G}'(z_b) & 0 \\ -g\mathcal{G}'(z_a) & -\varepsilon & 0 & 0 \\ -\beta\mathcal{G}'(z_a) & 0 & -(1+w\mathcal{G}'(z_b)) & \varepsilon \\ 0 & 0 & -g\mathcal{G}'(z_b) & -\varepsilon \end{pmatrix}. \tag{2.14}$$

Note that ζ has negative real part eigenvalues if and only if $\hat{\zeta}$ has negative real part eigenvalues.

Observe that when $\varepsilon = 0$, $\hat{\zeta}$ has two zero eigenvalues with eigenvectors $v_1 = (0,1,0,0)^t$ and $v_2 = (0,0,0,1)^t$. Rewrite $\hat{\zeta}$ in the basis $\{v_1, v_2, v_3, v_4\}$, where $v_3 = (1,0,0,0)^t$ and $v_4 = (0,0,1,0)^t$. In this basis, $\hat{\zeta}$ has the form

$$\tilde{\zeta} = \begin{pmatrix} -\varepsilon I_2 & A \\ \varepsilon I_2 & B \end{pmatrix},$$

where

$$A = \begin{pmatrix} -g\mathcal{G}'(z_a) & 0 \\ 0 & -g\mathcal{G}'(z_b) \end{pmatrix} \quad \text{and} \quad B = \begin{pmatrix} -(1+w\mathcal{G}'(z_a)) & -\beta\mathcal{G}'(z_b) \\ -\beta\mathcal{G}'(z_a) & -(1+w\mathcal{G}'(z_b)) \end{pmatrix}.$$

So we need to discuss when the eigenvalues of $\tilde{\zeta}$ all have negative real part.

Proof of part (a). If we assume that the eigenvalues of $\tilde{\zeta}$ have negative real part for all $\varepsilon \approx 0$, then the eigenvalues of B must have negative real part. Note that $\operatorname{tr}(B) < 0$; so the eigenvalues of B have negative real part if and only if

$$\det(B) = 1 + w(\mathcal{G}'(z_a) + \mathcal{G}'(z_b)) + (w^2 - \beta^2)\mathcal{G}'(z_a)\mathcal{G}'(z_b) > 0. \tag{2.15}$$

The inequality $\det(B) > 0$ can be rewritten as

$$\left(\frac{1}{\mathcal{G}'(z_a)} + w\right)\left(\frac{1}{\mathcal{G}'(z_b)} + w\right) > \beta^2. \tag{2.16}$$

Since we evaluate the Jacobian at all points in $\mathcal{S}$, the points z_a and z_b are arbitrary. Hence, the minimum of the left-hand side of (2.16) must be greater than β^2, and that minimum is

$$\left(\frac{1}{\mathcal{G}'(z_{max})} + w\right)^2 > \beta^2.$$

Upon taking square roots, we have

$$\beta < \frac{1}{\mathcal{G}'(z_{max})} + w. \tag{2.17}$$

So if all eigenvalues of $\tilde{\zeta}$ have negative real part, then (2.1) must hold.

Proof of part (b). We assume (2.17) is valid. If $\varepsilon > 0$ and $g = 0$, then $\tilde{\zeta}$ is block lower triangular and all of its eigenvalues have negative real part. Continuity of eigenvalues implies that the converse can fail only if there is a point in $\mathcal{S}$ for which $\tilde{\zeta}$ has an eigenvalue on the imaginary axis, that is, an eigenvalue of the form τi. We show that this is not possible. Let

$$P(\lambda) = \lambda^4 + p\lambda^3 + q\lambda^2 + r\lambda + s$$

be the characteristic polynomial of $\tilde{\zeta}$, where

$$s = \det(\tilde{\zeta}) = \varepsilon^2(\det(B) + g(\mathcal{G}'(z_a) + \mathcal{G}'(z_b)) + (g^2 + 2gw)\mathcal{G}'(z_a)\mathcal{G}'(z_b)) > 0$$

by (2.15). It follows that 0 is not an eigenvalue when (2.15) is satisfied.

If $\tilde{\zeta}$ has an eigenvalue $i\tau$, where $\tau \neq 0$, then

$$0 = P(i\tau) = \tau^4 - p\tau^3 i + q\tau^2 + r\tau i + s.$$

Equating real and imaginary parts yields $\tau^2 = r/p$ and $pqr - r^2 - sp^2 = 0$. We show that

$$pqr - r^2 - sp^2 > 0, \tag{2.18}$$

and hence $\tilde{\zeta}$ does not have pure imaginary eigenvalues. Tedious calculations verified by *Mathematica* show that

$$\begin{aligned} P(\lambda) = \lambda^4 &+ \left(2\varepsilon + 2 + w(\mathcal{G}'(z_a) + \mathcal{G}'(z_b)\right)\lambda^3 \\ &+ \left(\det(B) + 4\varepsilon + \varepsilon^2 + (2w + g)\varepsilon(\mathcal{G}'(z_a) + \mathcal{G}'(z_b))\right)\lambda^2 \\ &+ \varepsilon\left(2\det(B) + 2\varepsilon + (w\varepsilon + g(1+\varepsilon))(\mathcal{G}'(z_a) + \mathcal{G}'(z_b)) + 2wg\mathcal{G}'(z_a)\mathcal{G}'(z_b)\right)\lambda \\ &+ \varepsilon^2(\det(B) + g(\mathcal{G}'(z_a) + \mathcal{G}'(z_b)) + (g^2 + 2gw)\mathcal{G}'(z_a)\mathcal{G}'(z_b)) \end{aligned}$$

and

$$pqr - r^2 - sp^2 = \varepsilon\gamma_2 \det(B) + 2\varepsilon\gamma_1\left[\det(B) + \varepsilon\left(\varepsilon + \gamma_1\right)\right]^2 + \varepsilon^2\left(\gamma_2(\varepsilon + \gamma_1) + \gamma_3\right),$$

where

$$\begin{aligned}\gamma_1 &= 2 + w(\mathcal{G}'(z_a) + \mathcal{G}'(z_b)),\\ \gamma_2 &= 2g(1+\varepsilon)^2(\mathcal{G}'(z_a) + \mathcal{G}'(z_b)) + gw(1+3\varepsilon)(\mathcal{G}'(z_a)^2 + \mathcal{G}'(z_b)^2)\\ &\quad + 2gw(1+\varepsilon+\gamma_1)\mathcal{G}'(z_a)\mathcal{G}'(z_b),\\ \gamma_3 &= g^2\left(\mathcal{G}'(z_a) - \mathcal{G}'(z_b)\right)^2(\mathcal{G}'(z_a)\,w + \varepsilon + 1)(\mathcal{G}'(z_b)\,w + \varepsilon + 1).\end{aligned}$$

Since $\gamma_1, \gamma_2, \gamma_3$ are all positive, condition (2.18) is satisfied whenever $\det(B) > 0$. ■

3. Bifurcations from fusion.

In this section we discuss steady-state and Hopf bifurcations from synchronous equilibria for a smooth gain function, showing how symmetry-breaking TB bifurcations and their universal unfoldings occur.

3.1. Bifurcations from fusion in two-cell reduction (1.2).

We show that steady-state (saddle-node) bifurcations to synchronous equilibria occur only when the synchronous state is unstable and that steady-state (pitchfork) bifurcations to asynchronous equilibria can occur from a stable synchronous equilibrium. We also see how bifurcation from synchronous and asynchronous equilibria leads to rivalry and WTA regimes. These calculations are similar to those in Curtu et al. (2008), but are needed to identify TB points.

Synchronous equilibria of the two-cell system (1.2). Recall that (1.2) has the coupled system form

$$\begin{aligned}\dot{a} &= \mathcal{A}(a,b),\\ \dot{b} &= \mathcal{A}(b,a),\end{aligned} \tag{3.1}$$

where $a = (a^E, a^H)$ and $b = (b^E, b^H)$. Moreover, systems (3.1) have the transpositional symmetry

$$\tau(a,b) = (b,a). \tag{3.2}$$

Synchronous states satisfy $b = a$.

Specifically, equilibria of (1.2) satisfy $a^E = a^H$ and $b^E = b^H$, and synchronous equilibria also satisfy $x \equiv a^E = b^E = a^H = b^H \geq 0$. It then follows from (1.2) that

$$x = \mathcal{G}\left(I + \rho x\right), \tag{3.3}$$

where

$$\rho \equiv \alpha_0 - \beta - g. \tag{3.4}$$

Lemma 3.1. *Suppose $\mathcal{G}$ is conforming with threshold θ. If $I > \theta$, then (3.3) has a unique solution when $\rho \leq 0$ and has one to three solutions when $\rho > 0$.*

Proof. First note that when $I + \rho x \leq \theta$, (3.3) has no solution. The reason is that, on the one hand, $x = \mathcal{G}(I + \rho x) = 0$; whereas, on the other hand, when $x = 0$ and $I > \theta$, $\mathcal{G}(I + \rho x) = \mathcal{G}(I) > 0$, which is a contradiction. So we can assume that $I + \rho x > \theta$.

Observe that solving (3.3) is equivalent to solving

$$\varphi(x) \equiv \mathcal{G}(I + \rho x) - x = 0 \tag{3.5}$$

when $x \geq 0$. Note that

$$\varphi'(x) = \rho\mathcal{G}'(I + \rho x) - 1 \qquad \text{and} \qquad \varphi''(x) = \rho^2\mathcal{G}''(I + \rho x). \tag{3.6}$$

We claim that $\varphi = 0$ has at most three solutions. Suppose $\varphi(x) = 0$ has four solutions. Then smoothness of $\mathcal{G}$ implies that φ' has three zeros and $\varphi'' = \rho^2\mathcal{G}''$ has two zeros in the range $I + \rho x > \theta$, which contradicts the assumption that $\mathcal{G}$ is conforming.

Finally, we show that (3.5) has a unique solution when $\rho \leq 0$. When $\rho = 0$ the only solution to (3.5) is $x = \mathcal{G}(I)$. Hence, we can assume $\rho < 0$. Note that (3.6) implies that $\varphi'(x) < 0$ for all x and that φ is strictly decreasing. It follows that $\varphi = 0$ has at most one solution. Since

$$\varphi(0) = \mathcal{G}(I) > 0 \quad \text{and} \quad \varphi\left(-\frac{I-\theta}{\rho}\right) = \mathcal{G}(\theta) + \frac{I-\theta}{\rho} = \frac{I-\theta}{\rho} < 0,$$

it follows that (3.3) has a unique solution and that this solution is in $(0, -\frac{I-\theta}{\rho})$. ∎

Let x_0 be a solution to (3.3) and write

$$z_0 = I + \rho x_0.$$

Then z_0 is a solution of

$$z_0 = I + \rho\mathcal{G}(z_0). \tag{3.7}$$

It then follows from the proof of Lemma 3.1 that

$$z_0 > \theta \tag{3.8}$$

whenever $x_0 > 0$ corresponds to a synchronous equilibrium, that is, a solution to (3.3).

Bifurcations from synchronous equilibria of (1.2). Next we discuss the Jacobian of (1.2) at a synchronous equilibrium corresponding to a solution z_0 of (3.7). It follows from symmetry that the Jacobian of (3.1) at a synchronous equilibrium has the form

$$J = \begin{pmatrix} \Lambda & \Delta \\ \Delta & \Lambda \end{pmatrix}, \tag{3.9}$$

where $\Lambda = (D_1(\mathcal{A})(a, a)$ is the linearized internal dynamics and $\Delta = (D_2\mathcal{A})(a, a)$ is the linearized coupling. The eigenvalues of J are given by the eigenvalues of the 2×2 matrices $\Lambda \pm \Delta$. Note that the eigenvalues of $\Lambda + \Delta$ have synchronous eigenvectors $(v, v)^t$. Furthermore, saddle-node bifurcations typically occur when these eigenvalues pass through zero, whereas the eigenvalues of $\Lambda - \Delta$ have asynchronous eigenvectors $(v, -v)^t$, and, because of symmetry, pitchfork bifurcations typically occur when these eigenvalues pass through zero.

A calculation shows

$$\Lambda = \frac{1}{\varepsilon}\begin{pmatrix} -1+\alpha_0\mathcal{G}'(z_0) & -g\mathcal{G}'(z_0) \\ \varepsilon & -\varepsilon \end{pmatrix}$$

and

$$\Delta = \frac{1}{\varepsilon}\begin{pmatrix} -\beta\mathcal{G}'(z_0) & 0 \\ 0 & 0 \end{pmatrix}.$$

Thus, the eigenvalues in the synchronous and asynchronous directions are the eigenvalues of the matrices

$$\Lambda \pm \Delta = \frac{1}{\varepsilon}\begin{pmatrix} -1+(\alpha_0 \mp \beta)\mathcal{G}'(z_0) & -g\mathcal{G}'(z_0) \\ \varepsilon & -\varepsilon \end{pmatrix}. \tag{3.10}$$

The traces and determinants of the above matrices in the synchronous and asynchronous directions are

$$\operatorname{tr}(\Lambda+\Delta) = \frac{-1-\varepsilon+(\alpha_0-\beta)\mathcal{G}'(z_0)}{\varepsilon}, \tag{3.11}$$

$$\det(\Lambda+\Delta) = \frac{1-(\alpha_0-\beta-g)\mathcal{G}'(z_0)}{\varepsilon}, \tag{3.12}$$

$$\operatorname{tr}(\Lambda-\Delta) = \frac{-1-\varepsilon+(\alpha_0+\beta)\mathcal{G}'(z_0)}{\varepsilon}, \tag{3.13}$$

$$\det(\Lambda-\Delta) = \frac{1-(\alpha_0+\beta-g)\mathcal{G}'(z_0)}{\varepsilon}. \tag{3.14}$$

Remark 3.2. The stability of a synchronous equilibrium is determined by the signs of the real parts of the eigenvalues in the asynchronous directions. To see this, use (3.11)–(3.14) to compute

$$\begin{array}{rcccl} \det(\Lambda-\Delta) & = & \det(\Lambda+\Delta) - \frac{2\beta\mathcal{G}'(z_0)}{\varepsilon} & < & \det(\Lambda+\Delta), \\ \operatorname{tr}(\Lambda+\Delta) & = & \operatorname{tr}(\Lambda-\Delta) - \frac{2\beta\mathcal{G}'(z_0)}{\varepsilon} & < & \operatorname{tr}(\Lambda-\Delta) \end{array}$$

since $\beta > 0$, $\mathcal{G}'(x) \geq 0$. Either the asynchronous directions are both stable or one is unstable. If one is unstable, then the synchronous equilibrium is unstable. If they are both stable, then

$$\begin{array}{rcccl} 0 & < & \det(\Lambda-\Delta) & < & \det(\Lambda+\Delta), \\ 0 & > & \operatorname{tr}(\Lambda-\Delta) & > & \operatorname{tr}(\Lambda+\Delta) \end{array}$$

and the eigenvalues in the synchronous directions are also stable. ■

Remark 3.3. It follows from Remark 3.2 that a synchrony-preserving steady-state bifurcation (that is, $\det(\Lambda+\Delta)=0$) can occur only from an unstable synchronous equilibrium since $\det(\Lambda-\Delta)<0$. Similarly, a synchrony-preserving Hopf bifurcation (that is, $\det(\Lambda+\Delta)>0$ and $\operatorname{tr}(\Lambda+\Delta)=0$) can also occur only from an unstable synchronous equilibrium since $\operatorname{tr}(\Lambda-\Delta)>0$. Thus, if these bifurcations exist, they must lead to unstable solutions.

In addition, a synchrony-breaking Hopf bifurcation can occur only from a stable synchronous equilibrium. To see this, observe that the eigenvalues of $\Lambda+\Delta$ have negative real part, since $\det(\Lambda+\Delta) > \det(\Lambda-\Delta) > 0$ and $\operatorname{tr}(\Lambda+\Delta) < \operatorname{tr}(\Lambda-\Delta) = 0$. ■

To summarize, steady-state bifurcation from a stable synchronous equilibrium can occur only via a synchrony-breaking bifurcation to a WTA state. Hopf bifurcation from a stable synchronous equilibrium can occur only via a synchrony-breaking bifurcation to a rivalry state. Conditions for these bifurcations are given by (3.7) and

$$\text{steady-state branching (onset of WTA): } 1-(\alpha_0+\beta-g)\mathcal{G}'(z_0)=0, \tag{3.15}$$

$$\text{Hopf bifurcation (onset of rivalry): } -1-\varepsilon+(\alpha_0+\beta)\mathcal{G}'(z_0)=0. \tag{3.16}$$

3.2. Symmetry-breaking Takens–Bogdanov bifurcation. A TB bifurcation occurs when then Jacobian has a double zero eigenvalue with a single null vector. In a coupled system of the form (3.1) such a bifurcation can occur from a synchronous equilibrium either in the synchronous or in the asynchronous directions. It follows from Remark 3.3 that a TB bifurcation from a stable synchronous equilibrium can occur in (1.2) only in the asynchronous directions, that is, when the trace and determinant of $\Lambda-\Delta$ are both zero. Note that such a TB bifurcation is symmetry-breaking and is not the standard codimension two bifurcation. This symmetry-breaking bifurcation has been studied in Takens (1974); see also A TB bifurcation occurs when then Jacobian has a double zero eigenvalue with a single null vector. In a coupled system of the form (3.1) such a bifurcation can occur from a synchronous equilibrium either in the synchronous or in the asynchronous directions. It follows from Remark 3.3 that a TB bifurcation from a stable synchronous equilibrium can occur in (1.2) only in the asynchronous directions, that is, when the trace and determinant of $\Lambda-\Delta$ are both zero. Note that such a TB bifurcation is symmetry-breaking and is not the standard codimension two bifurcation. This symmetry-breaking bifurcation has been studied in Takens (1974); see also section 7 of Guckenheimer and Holmes (1983).

Note that the transposition symmetry τ in (3.2) acts on the center subspace (the asynchronous directions) as $-I_2$. It follows that the center manifold vector field associated to a symmetry-breaking TB bifurcation is an odd function, which is not the case in standard TB bifurcation. A (truncated) universal unfolding of a synchrony-breaking TB bifurcation has the form

$$\begin{aligned}\dot{y}_1 &= y_2,\\ \dot{y}_2 &= \mu_1 y_1+\mu_2 y_2+\delta y_1^3+\eta y_1^2 y_2.\end{aligned} \tag{3.17}$$

(Note that the cubic monomials other than y_1^3 and $y_1^2y_2$ in the $\dot{y}_2$ equation can be eliminated by near-identity transformation.) Thus, near the TB bifurcation point and modulo higher order terms, the four-dimensional system (1.2) may be reduced via center manifold reduction and normal form derivation (Guckenheimer and Holmes (1983)) to a system of the form (3.17).

Solution types in unfoldings of Takens–Bogdanov singularities. The qualitative behavior of solutions to (3.17) depends on the signs of δ and η as described in Guckenheimer and Holmes (1983). Up to time reversal, there are two cases to consider: $\delta<0$, $\eta<0$ and $\delta>0$, $\eta<0$. Figure 5 shows the $\mu_1\mu_2$ bifurcation diagrams for these two cases. In this section, we review the case when $\delta<0$ and $\eta<0$ (Figure 5 (left)) and show numerically that this is the case related to our study.

We identify six connected regions where the behavior of the system is qualitatively the same for parameters within each region and qualitatively different for parameters in different

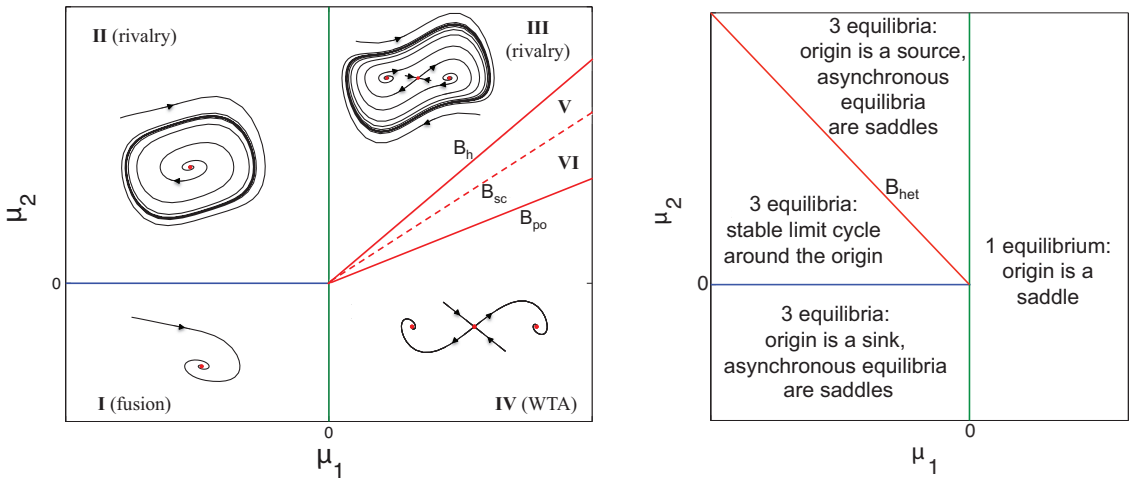

Figure 5. *Bifurcation set for* (3.17). *Left:* $\delta < 0$, $\eta < 0$. *Right:* $\delta > 0$, $\eta < 0$.

regions. When $\mu_1 < 0$, the only equilibrium is at the origin. In Region I ($\mu_1 < 0$, $\mu_2 < 0$) the origin is a sink. A Hopf bifurcation takes place at $\mu_1 < 0$, $\mu_2 = 0$, producing a stable limit cycle in Region II ($\mu_1 < 0$, $\mu_2 > 0$). When $\mu_1 = 0$, a pitchfork bifurcation occurs. When $\mu_2 > 0$, this bifurcation leads to a saddle and two sources in Region III (surrounded by a stable limit cycle) and when $\mu_2 < 0$, the bifurcation leads to a saddle and two sinks in Region IV. On the ray B_h given by

$$\mu_2 = \frac{\eta}{\delta}\mu_1 \quad \text{with} \quad \mu_1 > 0,$$

a subcritical Hopf bifurcation occurs, and two unstable limit cycles appear in Region V near and below B_h. These unstable limit cycles are surrounded by a stable limit cycle. When decreasing μ_2, the two unstable limit cycles in Region V merge to an unstable limit cycle in Region VI via a homoclinic (or glueing) bifurcation. Further decreasing of μ_2 leads to the disappearance of the unstable and stable limit cycles in a saddle-node of periodic solutions bifurcation. The curve B_{sc} in Figure 5 (left) denotes homoclinic bifurcation points, and the curve B_{po} denotes points where saddle-nodes of periodic solutions occur. Note that in Regions V and VI, stable WTA and rivalry coexist. See Figure 6.

3.3. Existence of Takens–Bogdanov points in two-cell reduction. Next we show that TB singularities occur in the two-cell quotient network equations (1.2).

Proposition 3.4. *A symmetry-breaking TB singularity occurs at the synchronous equilibrium associated to z^* in the two-cell system equations* (1.2) *at positive parameter values $I^*, \alpha_0^* = (n-1)w^*, \beta^*, g^*, \varepsilon^*$ if z^* satisfies*

$$z_0^* = I^* + (\alpha_0^* - \beta^* - g^*)\mathcal{G}(z_0^*) \tag{3.18}$$

and the other parameters satisfy

$$\varepsilon^* = \frac{g^*}{\alpha_0^* + \beta^* - g^*}, \tag{3.19}$$

$$1 - (\alpha_0^* + \beta^* - g^*)\mathcal{G}'(z_0^*) = 0. \tag{3.20}$$

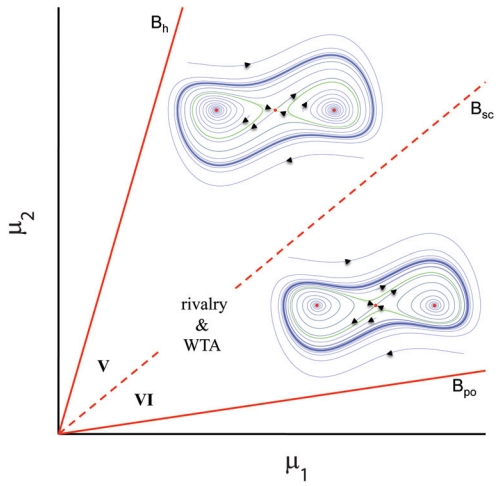

Figure 6. *Phase portraits of regions* V *and* VI *in Figure 5 when* $\delta < 0$, $\eta < 0$.

We remark that (3.20) implies that

$$\nu^* \equiv \alpha_0^* - g^* = \frac{1}{\mathcal{G}'(z_0^*)} - \beta^*. \tag{3.21}$$

Proof. Such bifurcations are found by solving (3.7), (3.15), and (3.16) simultaneously. Note that ε appears only in (3.16) and a calculation shows that we can replace (3.16) by (3.19). If (3.21) is valid, then $\varepsilon^* > 0$. It follows that there exists a double zero eigenvalue for any combination of parameters for which there is a steady-state branching; that is, (3.7) (i.e., (3.18)) and (3.15) (i.e., (3.20)) are satisfied.

Note that the matrix in (3.10) is never identically zero. This implies that there is only one eigenvector for a zero eigenvalue, and hence that $\Lambda - \Delta$ is nilpotent at the double zero eigenvalue. ∎

It remains to show that conditions for existence of a TB singularity given in Proposition 3.4 can be simultaneously satisfied. We verify this point by showing that in fact the TB points in the two-cell case lie on a three-parameter surface (parameterized by z^*, β^*, g^*).

1. Choose $z_0^* > \theta$, which is necessary by (3.8).
2. Choose
$$\beta^* > \frac{1}{2}\left(\frac{1}{\mathcal{G}'(z_0^*)} - \frac{z_0^*}{\mathcal{G}(z_0^*)}\right).$$
3. Set
$$\nu^* = \frac{1}{\mathcal{G}'(z_0^*)} - \beta^*,$$
which is necessary by (3.21).
4. Choose
$$g^* > \max(0, -\nu^*),$$
which is clearly positive.

5. Set
$$\varepsilon^* = \frac{g^*}{\nu^* + \beta^*},$$
which is positive by step 3.
6. Set
$$\alpha_0^* = \nu^* + g^*,$$
which is positive by step 4.
7. Set
$$I^* = z_0^* - (\nu^* - \beta^*)\mathcal{G}(z_0^*).$$

It remains only to show that $I^* > 0$. Use step 3 to see that

$$z_0^* - (\nu^* - \beta^*)\mathcal{G}(z_0^*) = z^* - \left(\frac{1}{\mathcal{G}'(z_0^*)} - 2\beta^*\right)\mathcal{G}(z_0^*).$$

Observe that

$$z_0^* - \left(\frac{1}{\mathcal{G}'(z_0^*)} - 2\beta^*\right)\mathcal{G}(z_0^*) > 0$$

if and only if step 2 is satisfied. Finally, observe that step 5 implies (3.19), step 7 implies (3.18), and step 3 implies (3.20).

3.4. Existence of Takens–Bogdanov points in three-cell reduction. The three-cell quotient network equations (1.4) have the form

$$\begin{array}{rcl} \dot{a} &=& \mathcal{A}(a,b,c), \\ \dot{b} &=& \mathcal{A}(b,a,c), \\ \dot{c} &=& \mathcal{C}(c,a,b), \end{array} \tag{3.22}$$

where $\mathcal{C}(c,a,b) = \mathcal{C}(c,b,a)$. Specifically,

$$\mathcal{A}(a,b,c) = \begin{pmatrix} \frac{1}{\varepsilon}[-a^E + \mathcal{G}(I + (n-k-1)wa^E + kwc^E - \beta b^E - ga^H)] \\ a^E - a^H \end{pmatrix}$$

and

$$\mathcal{C}(c,a,b) = \begin{pmatrix} \frac{1}{\varepsilon}[-c^E + \mathcal{G}(I + (k-1)wc^E + (n-k)w(a^E + b^E) - gc^H)] \\ c^E - c^H \end{pmatrix}.$$

A synchronous equilibrium (a,a,c) satisfies $x \equiv a^E = b^E = a^H = b^H$ and $y \equiv c^E = c^H$, where (x,y) is a solution to

$$\begin{array}{rcl} x &=& \mathcal{G}(I + ((n-k-1)w - \beta - g)x + kwy), \\ y &=& \mathcal{G}(I + ((k-1)w - g)y + 2(n-k)wx). \end{array} \tag{3.23}$$

For ease of notation, we set

$$\begin{array}{rcl} z_0 &=& I + ((n-k-1)w - \beta - g)x + kwy, \\ u_0 &=& I + ((k-1)w - g)y + 2(n-k)wx. \end{array} \tag{3.24}$$

Using (3.24) it follows that (3.23) is equivalent to

$$\begin{aligned} z_0 &= I + ((n-k-1)w - \beta - g)\mathcal{G}(z_0) + kw\mathcal{G}(u_0), \\ u_0 &= I + 2(n-k)w\mathcal{G}(z_0) + ((k-1)w - g)\mathcal{G}(u_0). \end{aligned} \tag{3.25}$$

Proposition 3.5. *A symmetry-breaking TB singularity occurs at the synchronous equilibrium associated to z^*, u^* in the three-cell quotient equations (1.4) at positive parameter values $I^*, w^*, \beta^*, g^*, \varepsilon^*$ if z^*, u^* satisfies*

$$\begin{aligned} z_0^* &= I^* + ((n-k-1)w^* - \beta^* - g^*)\mathcal{G}(z_0^*) + kw^*\mathcal{G}(u_0^*), \\ u_0^* &= I^* + 2(n-k)w^*\mathcal{G}(z_0^*) + ((k-1)w^* - g^*)\mathcal{G}(u_0^*), \end{aligned} \tag{3.26}$$

where

$$\varepsilon^* = \frac{g^*}{\alpha_k^* + \beta^* - g^*}, \tag{3.27}$$

$$1 - (\alpha_k^* + \beta^* - g^*)\mathcal{G}'(z_0^*) = 0. \tag{3.28}$$

Proof. The quotient network has $\mathbf{Z}_2$ symmetry generated by τ. Then

$$\mathrm{Fix}(\tau) = \{(a, a, c)\} \qquad \text{and} \qquad \mathrm{Fix}(\tau)^\perp = \{(a, -a, 0)\}.$$

The Jacobian matrix of the system (3.22) at a synchronous equilibrium $(a, a, c) = (x, x, x, x, y, y)$ has the 2×2 block form

$$J = \begin{pmatrix} D_1\mathcal{A} & D_2\mathcal{A} & D_3\mathcal{A} \\ D_2\mathcal{A} & D_1\mathcal{A} & D_3\mathcal{A} \\ D_2\mathcal{C} & D_2\mathcal{C} & D_1\mathcal{C} \end{pmatrix}$$

and

$$J|\mathrm{Fix}(\tau)^\perp = D_1\mathcal{A} - D_2\mathcal{A}.$$

Since

$$D_1\mathcal{A} = \frac{1}{\varepsilon}\begin{pmatrix} -1 + \alpha_k\mathcal{G}'(z_0) & -g\mathcal{G}'(z_0) \\ \varepsilon & -\varepsilon \end{pmatrix}$$

and

$$D_2\mathcal{A} = \frac{1}{\varepsilon}\begin{pmatrix} -\beta\mathcal{G}'(z_0) & 0 \\ 0 & 0 \end{pmatrix},$$

where

$$\gamma = kw, \qquad z_0 = I + (\alpha_k - \beta - g)x + \gamma y,$$

we have that

$$D_1\mathcal{A} - D_2\mathcal{A} = \frac{1}{\varepsilon}\begin{pmatrix} -1 + (\alpha_k + \beta)\mathcal{G}'(z_0) & -g\mathcal{G}'(z_0) \\ \varepsilon & -\varepsilon \end{pmatrix}. \tag{3.29}$$

Note that $D_1\mathcal{A}-D_2\mathcal{A}$ is independent of γ and has the same expression as the two-cell quotient network. Since a TB singularity will occur when the determinant and the trace of $D_1\mathcal{A}-D_2\mathcal{A}$ vanish, Proposition 3.5 follows from the two-cell case. ■

Remark 3.6. To determine existence and stability of the TB point in the three-cell system we need to compute the eigenvalues of the Jacobian of three-cell quotient equations (1.4) whose eigenvectors lie in $\mathrm{Fix}(\tau)$. These eigenvalues are the eigenvalues of the matrix

$$J|\mathrm{Fix}(\tau) = \begin{pmatrix} D_1\mathcal{A}+D_2\mathcal{A} & D_3\mathcal{A} \\ 2D_2\mathcal{C} & D_1\mathcal{C} \end{pmatrix}.$$

The eigenvalues need to have nonzero real part in order to have existence of a TB point, and the eigenvalues have to have negative real part for the TB point to be stable. ■

Illustrative example for Proposition 3.5. We provide numerical results that verify the existence of TB points in the three-cell quotient network formed from a five-attribute system with two active cells in common ($n = 5$, $k = 2$). We note that in these computations, for convenience, we use the sigmoidal gain function (4.9), which does not satisfy the condition $\mathcal{G}'(z) = 0$ for $z < 0$ as required in Definition 1.1(c). Figure 7 shows a bifurcation diagram computed with XPPAUT confirming a TB singularity at certain parameter values. This TB point is stable in the $\mathrm{Fix}(\tau)$ directions in the six-dimensional quotient, as the eigenvalues of $J|\mathrm{Fix}(\tau)$ evaluated at the TB point have negative real part.

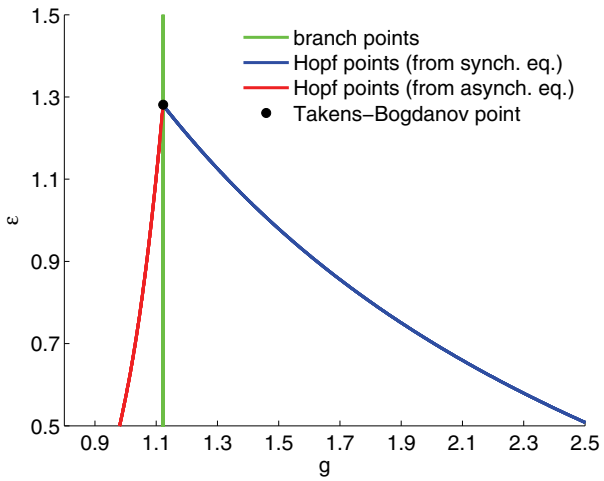

Figure 7. *Two-parameter bifurcation diagram indicating a TB singularity in the three-cell reduction* (1.4) *at* $g = 1.123$, $\varepsilon = 1.281$. *In these computations we set* $w^* = 0.25$, $\beta^* = 1.5$, *and* $I^* = 1$ *and calculate* $z^* = 0.763$ *and* $u^* = 0.934$.

3.5. Transverse stability of subspace $\mathcal{S}$ at Takens–Bogdanov points.

We have discussed the existence of symmetry-breaking TB points in the two- and three-cell quotient networks. Now we address the stability of these singularities in directions transverse to $\mathcal{S}$ in both the two- and three-cell reductions.

Theorem 3.7. *Suppose that z_0^* (as in (3.7)) is associated to a symmetry-breaking TB point X in either the two- or the three-cell quotient network. Then $\mathcal{S}$ is locally attracting at X.*

Proof. Note that $X \in \mathrm{Fix}(\tau)$. It follows from Proposition 2.8 that we must show that the traces of the 2×2 matrices ξ and $\phi \pm \psi$ are negative and the determinants are positive, where

$$\phi \pm \psi = \begin{pmatrix} -\frac{1}{\varepsilon^*}(1+(w^* \pm \beta^*)\mathcal{G}'(z_0^*)) & 1 \\ -\frac{1}{\varepsilon^*} g^* \mathcal{G}'(z_0^*) & -1 \end{pmatrix}.$$

By Lemma 2.12, ξ has eigenvalues with negative real part. So we need to prove that $\phi \pm \psi$ have eigenvalues with negative real part.

Since $w^*, \beta^*, g^*, \mathcal{G}' \geq 0$,

$$\begin{aligned} \mathrm{tr}(\phi+\psi) &= -1 - \frac{1}{\varepsilon^*}(1+(w^*+\beta^*)\mathcal{G}'(z_0^*)) &< 0, \\ \det(\phi+\psi) &= \frac{1}{\varepsilon^*}(1+(w^*+\beta^*+g^*)\mathcal{G}'(z_0^*))+1 &> 0. \end{aligned}$$

So the eigenvalues of $\phi+\psi$ have negative real part at z_0^*.

Next, compute the trace and determinant of $\phi-\psi$ at a TB bifurcation point. Propositions 3.4 and 3.5 imply that in both two- and three-cell quotient networks the following two equalities are valid at a TB point:

$$\varepsilon^* = \frac{g^*}{\alpha_k^* + \beta^* - g^*}, \qquad \mathcal{G}'(z_0^*) = \frac{1}{\alpha_k^* + \beta^* - g^*}.$$

Hence,

$$\begin{aligned} \mathrm{tr}\,(\phi-\psi) &= -1 - \frac{1}{\varepsilon^*}\left(1+(w^*-\beta^*)\mathcal{G}'(z_0^*)\right) \\ &= \frac{1}{\varepsilon^*}(-\varepsilon^* - 1 + (\beta^* - w^*)\mathcal{G}'(z_0^*)) \\ &= \frac{1}{\varepsilon^*}\left(-\frac{g^*}{\alpha_k^*+\beta^*-g^*} - 1 + (\beta^*-w^*)\frac{1}{\alpha_k^*+\beta^*-g^*}\right) \\ &= \frac{1}{\varepsilon^*}\left(-\frac{\alpha_k^*+w^*}{\alpha_k^*+\beta^*-g^*}\right) \\ &< 0. \end{aligned}$$

The last inequality is valid because $\alpha_k^* + \beta^* - g^* > 0$ at a TB point and all other parameters

are greater than zero. Similarly,

$$\begin{aligned}\det(\phi-\psi) &= \frac{1}{\varepsilon^*}(1+(g^*+w^*-\beta^*)\mathcal{G}'(z_0^*))\\ &= \frac{1}{\varepsilon^*}\left(1+(g^*+w^*-\beta^*)\frac{1}{\alpha_k^*+\beta^*-g^*}\right)\\ &= \frac{1}{\varepsilon^*}\left(\frac{\alpha_k^*+w^*}{\alpha_k^*+\beta^*-g^*}\right)\\ &> 0.\end{aligned}$$

That is, the eigenvalues of $\phi \pm \psi$ have negative real part at z_0^*. ■

Lack of global validity of Takens–Bodganov unfolding. Curtu (2010) notes the existence of mixed-mode oscillations in the two-cell system with sigmoidal gain. Near a Hopf bifurcation from asynchronous equilibria (i.e., near where the system transitions from rivalry to WTA), one can observe small oscillations around one of the asynchronous equilibria whose amplitudes grow over time until the orbit jumps to near the other asynchronous equilibria, where the process is repeated. Such mixed-mode oscillations cannot occur in the planar unfolding of the TB singularity. Hence, the TB singularity is not an organizing center for the global dynamics.

4. Unfoldings in two- and three-cell reductions. In this section we study the qualitative behavior of solutions in the reduced system with the input I as a distinguished bifurcation parameter. We note that there is no unfolding theory for dynamic bifurcations with a distinguished parameter, although such a theory does exist for zeros of a mapping (Golubitsky and Schaeffer (1985)). Distinguished parameter bifurcation theory is equivalent to the study of paths through the universal unfolding of a singularity without a distinguished parameter (Chapter III, section 12 of Golubitsky and Schaeffer (1985); Montaldi (1994)). Nevertheless, enough is known about paths through unfoldings to allow us to formally recover many of the observations of Curtu et al. (2008) by considering a degenerate path through the universal unfolding of the two-dimensional symmetry-breaking TB singularity. This observation leads to the prediction of other bifurcation scenarios whose existence we verify numerically for specific parameter regimes in (1.2).

Relating system parameters α_k, g to unfolding parameters μ_1, μ_2. Let z^* be associated to a TB singularity for the two-cell model, and let (z^*, u^*) be associated to a TB singularity for the three-cell model at parameters α_k^*, β^*, g^*, ε^*, I^*. Using the implicit function theorem, solve (3.26) (or in the two-cell quotient solve (3.18)), which is independent of ε, for

$$z_0 = \zeta(I, \alpha_k, \beta, g)$$

with

$$\zeta(I^*, \alpha_k^*, \beta^*, g^*) = z_0^*.$$

Now we relate the parameters $\alpha, \beta, g, \varepsilon, I$ near $\alpha^*, \beta^*, g^*, \varepsilon^*, I^*$ in (1.2) to μ_1, μ_2. By (3.17) μ_1 is minus the product of the critical eigenvalues of the Jacobian along the branch of synchronous

equilibria, and μ_2 is the sum of these eigenvalues. Hence, to first order (in the deviation of the equilibrium from the TB singularity, that is, $z - z^*$),

$$\begin{aligned} \mu_1 &\approx -\det(\Xi), \\ \mu_2 &\approx \operatorname{tr}(\Xi), \end{aligned} \tag{4.1}$$

where in the two-cell quotient (see (3.10))

$$\Xi = \Lambda - \Delta = \frac{1}{\varepsilon}\begin{pmatrix} -1 + (\alpha_0 + \beta)\mathcal{G}'(z_0) & -g\mathcal{G}'(z_0) \\ \varepsilon & -\varepsilon \end{pmatrix}$$

and in the three-cell quotient (see (3.29))

$$\Xi = D_1\mathcal{A} - D_2\mathcal{A} = \frac{1}{\varepsilon}\begin{pmatrix} -1 + (\alpha_k + \beta)\mathcal{G}'(z_0) & -g\mathcal{G}'(z_0) \\ \varepsilon & -\varepsilon \end{pmatrix}.$$

Hence, to first order,

$$\begin{aligned} \mu_1 &= \frac{-1 + (\alpha_k + \beta - g)\mathcal{G}'(z)}{\varepsilon} + \cdots, \\ \mu_2 &= \frac{-1 - \varepsilon + (\alpha_k + \beta)\mathcal{G}'(z)}{\varepsilon} + \cdots. \end{aligned} \tag{4.2}$$

Proposition 4.1. *The parameters α_k and g are universal unfolding parameters of a TB singularity.*

Proof. We begin by showing that

$$\mathcal{M} = \begin{pmatrix} \mu_{1,r} & \mu_{2,r} \\ \mu_{1,s} & \mu_{2,s} \end{pmatrix}$$

is invertible at z_0^*, where r, s are two of the variables $\alpha_k, \beta, g, \varepsilon$ and the second subscript indicates partial differentiation.

It follows from (4.2) that to first order in $z_0 - z_0^*$, μ_1 and μ_2 satisfy

$$\mu_1 = B\mu_2 + A, \tag{4.3}$$

where

$$A = 1 - \frac{1+\varepsilon}{\varepsilon}\frac{g}{\alpha_k + \beta} = \frac{1}{\varepsilon(\alpha_k + \beta - g)}\left(\varepsilon - \frac{g}{\alpha_k + \beta - g}\right) \quad \text{and} \quad B = \frac{\alpha_k + \beta - g}{\alpha_k + \beta}.$$

Differentiating both sides of (4.3) with respect to r yields

$$\mu_{1,r} = B\mu_{2,r} + A_r$$

since $\mu_1 = \mu_2 = 0$ at the TB point. Let

$$D = \det(\mathcal{M})$$

with parameters set at the TB point. It follows that

$$D = \det \begin{pmatrix} A_r & \mu_{2,r} \\ A_s & \mu_{2,s} \end{pmatrix}. \tag{4.4}$$

Next, we assume $r = \alpha_k$ and $s = g$. Since μ_2 does not depend explicitly on g and $\mathcal{G}''(z_0^*) = 0$, it follows that $\mu_{2,g} = 0$ at the bifurcation point. Thus, D in (4.4) reduces to

$$D = -A_g \mu_{2,\alpha_k}.$$

Calculations show that

$$A_g = -\frac{1+\varepsilon^*}{\varepsilon^*}\frac{1}{\alpha_k^* + \beta^*} \neq 0 \qquad \text{and} \qquad \mu_{2,\alpha_k} = \frac{1}{\varepsilon^*}\mathcal{G}'(z_0^*) \neq 0.$$

It follows that $D \neq 0$ and that α_k and g are universal unfolding parameters. ■

Next we verify numerically that the dynamics of (1.2) includes a TB bifurcation point with $\delta < 0$, $\eta < 0$, as pictured in Figure 5. We choose parameters $I^* = 0.8006$, $\alpha_0^* = 1$, $\beta^* = 1.5$, $g^* = 1$, and $\varepsilon^* = 2/3$. We set (α_0, g) to trace a small circle around the TB bifurcation point, namely,

$$\alpha_0 = \alpha_0^* + 0.01\cos(2\pi\lambda) \qquad \text{and} \qquad g = g^* + 0.01\sin(2\pi\lambda). \tag{4.5}$$

We then vary λ from 0.5 to 1.5 and obtain the bifurcation diagram in Figure 8 with bifurcation parameter λ.

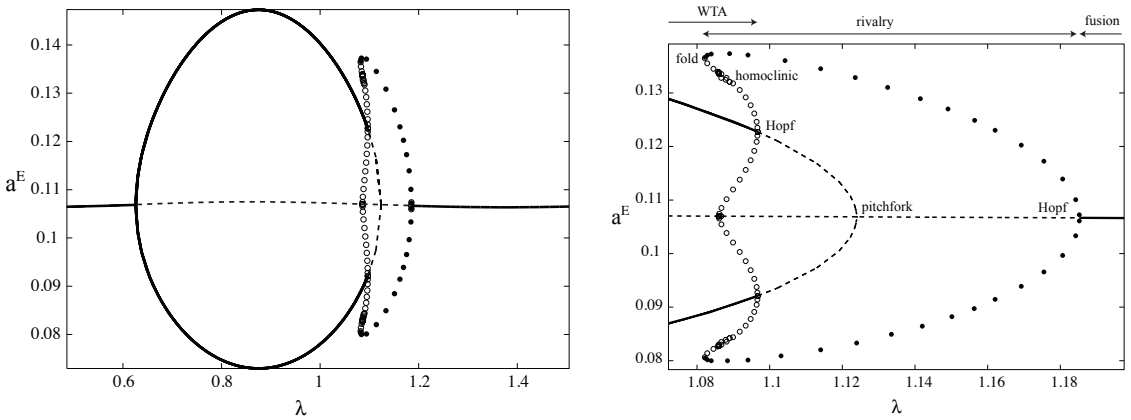

Figure 8. *Bifurcation diagram generated by a circle in the αg plane surrounding the point (α_0^*, g^*). A portion of the left panel is blown up on the right.*

From right to left (decreasing λ) in Figure 8, the following bifurcations occur in order: supercritical symmetry-breaking Hopf, symmetry-breaking pitchfork, subcritical asymmetric Hopf, homoclinic (to the fusion state, which is a saddle), and fold bifurcation (in the periodic solutions). This is exactly what happens in Figure 5 (left) when the path starts in Region I and wraps around the origin clockwise.

Singular variation of I. Numerical explorations of (1.2) and (1.4) lead to a symmetry-breaking pitchfork bifurcation and a symmetry-breaking Hopf bifurcation for small I and to another pair of these bifurcations for large I. See Figure 4 for the three-cell model and Curtu et al. (2008) for the two-cell model. It is reasonable to imagine each of these pairs of bifurcations coalescing into a TB bifurcation and to further imagine the two TB points themselves coalescing. At such a degeneracy in the variation of I, the trajectory $(\mu_1(I), \mu_2(I))$ in the unfolding space of the TB singularity must come up to the TB point and turn around. Hence, for some I^* the curve satisfies $(\mu_1'(I^*), \mu_2'(I^*)) = (0, 0)$. It follows from (4.2) that z_0^* must be at a point where $\mathcal{G}''(z_0^*) = 0$.

We assume that $\mathcal{G}$ is sigmoidal. It follows that there is a unique point $z_0^* = z_{max}$ such that $\mathcal{G}''(z_0^*) = 0$. Once z_0^* is chosen we can evaluate $\mathcal{G}(z_0^*)$ and $\mathcal{G}'(z_0^*)$. Then the equations obtained from conditions for TB bifurcation (3.18)–(3.20) can be solved as follows. Fix $\alpha_k^*, \beta^* > 0$ and solve sequentially for

$$g^* = \alpha_k^* + \beta^* - \frac{1}{\mathcal{G}'(z_0^*)}, \tag{4.6}$$

$$I^* = z_0^* + \left(2\beta^* - \frac{1}{\mathcal{G}'(z_0^*)}\right)\mathcal{G}(z_0^*), \tag{4.7}$$

and

$$\varepsilon^* = (\alpha_k^* + \beta^*)\mathcal{G}'(z_0^*) - 1. \tag{4.8}$$

For example, for the sigmoidal function

$$\mathcal{G}(x) = \frac{0.8}{1 + e^{-7.2(x-0.9)}}, \tag{4.9}$$

$\mathcal{G}''(0.9) = 0$. We can choose $\alpha_k^* = 0.157$, $\beta^* = 1$. Then by (4.6), (4.7), and (4.8), we get $g^* = 0.463$, $I^* = 1.42$, and $\varepsilon^* = \frac{2}{3}$.

Paths in the $\mu_1\mu_2$ plane as I varies. Unfolding theory suggests that a curve in the original parameter space corresponds to a curve in the $\mu_1\mu_2$ plane. We now consider the case where all parameters except the input I are fixed, and we consider I as a distinguished bifurcation parameter. It follows from (4.3) that the curve $(\mu_1(I), \mu_2(I))$ lies on the straight line whose slope is

$$\frac{\alpha_k + \beta}{\alpha_k + \beta - g}.$$

Moreover, we assume that the degeneracy condition $\mathcal{G}''(z_0^*) = 0$ holds.

When we fix the other parameters at $\alpha_k^*, \beta^*, g^*, \varepsilon^*$, the curve (approximately) traces the line and turns around at the origin; that is, $\mu_1(I^*) = \mu_2(I^*) = 0$ and $\mu_{1,I}(I^*) = \mu_{2,I}(I^*) = 0$. This conclusion follows from $\mathcal{G}''(z_0^*) = 0$; the degenerate path is illustrated as path 1 in Figure 9. Suppose that we now fix the other parameters at values near their * values; then the path generated by varying I will be a perturbation of the degenerate path and could in principle be any of those in Figure 9. Figure 10 gives examples where bifurcation diagrams corresponding to these paths occur in the original system (1.2). Note that Figure 10 (lower

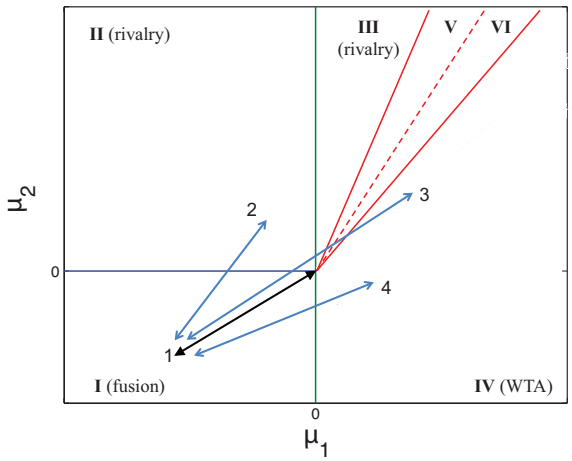

Figure 9. *Sample paths in $\mu_1\mu_2$ plane as I varies: path* 1 *is the degenerate path with parameters set at their * values; paths* 2, 3, 4 *are possible perturbations of this path. Path* 1: *fusion state, path traces a line that turns around at the origin. Path* 2: *states transition from fusion to rivalry. Path* 3: *fusion to rivalry, to states where rivalry and WTA are both stable, to WTA. Path* 4: *fusion to WTA. The slopes of the curves separating Regions* III, V, VI, *and* IV *depend on δ and η in the normal form* (3.17).

left) corresponds to path 3 in Figure 9 and is similar, but not identical, to Figure 3 in Curtu (2010). Consequently, we find regions in the input I with coexistence of a stable WTA and a stable rivalry state. There are other differences with more complex dynamics occurring in Curtu (2010).

5. Effect of recurrent excitation. In section 1 we noted that when one considers generalized rivalry, or rivalry between patterns, recurrent excitation arises naturally in the quotient network from reciprocal excitation in the original network. In this section we explore the effect recurrent excitation has on the dynamical states of the network. The amount of recurrent excitation depends on both the number of attributes n and the number of cells in common k. We show that if two patterns have no cells in common, then increasing the number of attributes causes the fusion state (or synchronous equilibrium) to lose stability at lower input signal strengths, leading to either rivalry or WTA. With a sufficiently large number of attributes, this loss of stability will lead to WTA. Increasing the number of cells in common can recover the transition from fusion to rivalry with a large number of attributes, and in general causes the fusion state to lose stability at higher input signal strengths.

Increasing number of attributes: No cells in common. We claim that in networks with no cells in common ($k = 0$) and with strong inhibition β, the fusion state is lost at lower values of the input strength I as the number of attributes n increases. We fix parameter values $\alpha_0, \beta, g, \varepsilon$ and the sigmoidal gain function $\mathcal{G}$ in (1.2) and let I_u denote the minimum value of I where the fusion state loses stability. Recall that in two-pattern networks with no cells in common $\alpha_0 = w(n-1)$ is the amount of recurrent excitation in the quotient network, where w is the strength of a single reciprocal excitatory connection in the original network. Specifically, we write I_u as a function of α_0 and prove the following proposition.

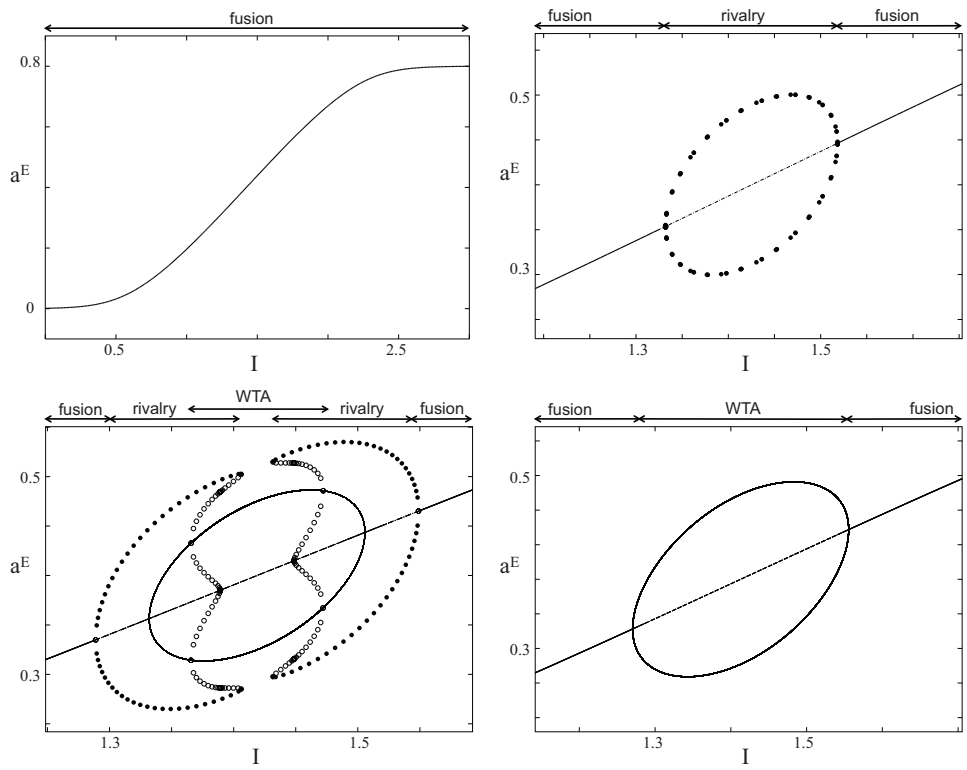

Figure 10. *Bifurcation diagrams in the original system (1.2) corresponding to the different paths through the $\mu_1\mu_2$ plane shown in Figure 9. In all panels, I is varied while $\beta = \beta^* = 1$ and $\varepsilon = \varepsilon^* = \frac{2}{3}$. Top left: $\alpha = \alpha_0^* = 0.157$, $g = g^* = 0.463$ (path 1). Top right: $\alpha = 1.1\alpha_0^*$, $g = 1.05g^*$ (path 2). Bottom left: $\alpha = 1.2\alpha_0^*$, $g = 1.05g^*$ (path 3). Bottom right: $\alpha = \alpha_0^*$, $g = 0.95g^*$ (path 4).*

Proposition 5.1. *For sigmoidal $\mathcal{G}$ and no cells in common, if the inhibition β is greater than the strength of self-adaptation g (that is, $\beta > g$), then I_u decreases as α_0 increases.*

Since inhibition is often assumed to be strong in these models, $\beta > g$ is typically the case. Our proof shows that both steady-state and Hopf bifurcation from the fusion state occur when α_0 is sufficiently large.

Proof. We need to show that $\frac{dI_u}{d\alpha_0} < 0$. Stable synchronous equilibria of (1.2), which correspond to fusion, lose stability through either a steady-state branching to WTA or a Hopf bifurcation to rivalry. Let $z(I_u)$ be the corresponding solution to (3.7) where the bifurcation takes place. Recall that the conditions for these bifurcations are given in (3.15) and (3.16), and can be rewritten as

$$\text{steady-state branching: } \mathcal{G}'(z(I_u)) = \frac{1}{\alpha_0 + \beta - g}, \tag{5.1}$$

$$\text{Hopf bifurcation: } \mathcal{G}'(z(I_u)) = \frac{1+\varepsilon}{\alpha_0 + \beta}. \tag{5.2}$$

Which of the two bifurcations occurs at a smaller value of I, and therefore is the one that leads to loss of stability of the synchronous equilibrium, depends on whether ε is greater or lesser

than the right-hand side of (3.19). It follows from Definition 1.1 that for sigmoidal functions $\mathcal{G}$, $\mathcal{G}'(z)$ has a maximum value at $z = z_{max}$, which is independent of parameters in the model, and $\lim_{z\to\pm\infty} \mathcal{G}'(z) = 0$. Hence, when α_0 is sufficiently large, it follows from (5.1) that there are exactly two values of I where steady-state bifurcation from the fusion state occurs and from (5.2) that there are exactly two values of I where Hopf bifurcation from the fusion state occurs.

First, we consider the case where

$$\varepsilon > \frac{g}{\alpha_0 + \beta - g},$$

so stability of the synchronous equilibrium is lost due to steady-state branching, and we show when $\frac{dI_u}{d\alpha_0} < 0$. Implicit differentiation of (5.1) yields

$$\mathcal{G}''(z(I_u))\frac{dz}{dI}(I_u)\frac{dI_u}{d\alpha_0} = -\frac{1}{(\alpha_0 + \beta - g)^2} < 0. \tag{5.3}$$

Hence $\frac{dI_u}{d\alpha_0} < 0$ when

$$\mathcal{G}''(z(I_u))\frac{dz}{dI}(I_u) > 0. \tag{5.4}$$

To verify (5.4), we show that $\mathcal{G}''(z(I_u)) > 0$ at the first instability, and then we show $\frac{dz}{dI}(I_u) > 0$ when $\alpha_0 + \beta > g$.

For a sigmoidal gain function, (5.1) will be satisfied at two different values of $z(I)$, one on each side of the z_{max}. The branching at the lower value of I is the one of interest here, as it represents loss of stability of the synchronous equilibrium as I is increased from zero. On this side of z_{max}, $\mathcal{G}''(z)$ is positive. Thus, (5.4) holds if $\frac{dz}{dI}$ is positive. From (5.1) and implicit differentiation of (3.7), at the bifurcation point we have

$$\frac{dz}{dI} = \frac{1}{1 - (\alpha_0 - \beta - g)\mathcal{G}'(z)} = \frac{\alpha_0 + \beta - g}{2\beta}. \tag{5.5}$$

So $\frac{dz}{dI} > 0$ as long as $\alpha_0 + \beta > g$, which follows from $\beta > g$.

The argument for the case

$$\varepsilon < \frac{g}{\alpha_0 + \beta - g}, \tag{5.6}$$

where stability of the synchronous equilibrium is lost due to Hopf bifurcation, follows the same logic as the case for steady-state branching. Implicit differentiation of (5.2) gives

$$\mathcal{G}''(z(I_u))\frac{dz}{dI}(I_u)\frac{dI_u}{d\alpha_0} = -\frac{1 + \varepsilon}{(\alpha_0 + \beta)^2} < 0. \tag{5.7}$$

We again have that $\frac{dI_u}{d\alpha_0} < 0$ when (5.4) is satisfied. The argument that $\mathcal{G}''(z) > 0$ is valid is identical to the argument given in the steady-state case. We complete the argument by showing that $\frac{dz}{dI} > 0$ at the first bifurcation.

From (5.5) and (5.2) we have that at the Hopf point

$$\frac{dz}{dI} = \frac{\alpha_0 + \beta}{2\beta + g - \varepsilon(\alpha_0 - \beta - g)}. \tag{5.8}$$

On the one hand, we see from the denominator of (5.8) that $\frac{dz}{dI}$ is positive when $\alpha_0 - \beta - g \leq 0$. On the other hand, if $\alpha_0 - \beta - g > 0$, then $\frac{dz}{dI} > 0$ when

$$\varepsilon < \frac{2\beta + g}{\alpha_0 - \beta - g}. \tag{5.9}$$

This condition is always satisfied when stability is lost due to Hopf bifurcation since

$$\frac{g}{\alpha_0 + \beta - g} < \frac{2\beta + g}{\alpha_0 - \beta - g}$$

when $\alpha_0 - \beta - g > 0$. ■

Remark 5.2. If the number of attributes is sufficiently large, then at I_u fusion will lose stability to WTA and not rivalry. This can be seen by considering (5.6), the condition that dictates when Hopf bifurcation from the synchronous equilibrium occurs before steady-state branching. Keeping the other parameters fixed, as n and therefore α_0 are increased, eventually (5.6) will not hold and steady-state branching will occur first. ■

Increasing the number of cells in common. We showed that increasing the number of attributes with no cells in common ($k = 0$) leads to the loss of stability of the fusion state at lower values of I, and that for sufficiently large n the transition will be to WTA. This makes sense intuitively. Suppose the number of attributes that are different between two patterns is increased. Then, we expect the network to require less input to transition to a state in which one pattern is chosen over the other. Here, we show that for fixed n, as the number of attributes in common is increased the network requires more input to exhibit rivalry or WTA; i.e., the fusion state loses stability at higher values of I.

Proposition 5.3. *For a fixed number of attributes and sigmoidal $\mathcal{G}$, if $\beta > g$, then I_u increases as the number of cells in common increases.*

Proof. We need to show that $\frac{dI_u}{dk} > 0$. When $k \geq 1$, we have the system (1.4) rather than (1.2). Steady-state bifurcation from the stable equilibria occurs when the determinant of $\mathbf{D}_1\mathcal{A} - D_2\mathcal{A}$ in (3.29) is zero, and Hopf bifurcation takes place when its trace is zero. That is, the conditions for bifurcation from the stable equilibrium in (1.4) are

$$\text{steady-state branching: } \mathcal{G}'(z(I_u)) = \frac{1}{\alpha_k + \beta - g}, \tag{5.10}$$

$$\text{Hopf bifurcation: } \mathcal{G}'(z(I_u)) = \frac{1 + \varepsilon}{\alpha_k + \beta}, \tag{5.11}$$

where $\alpha_k = w(n - k - 1)$. The relevant effect of increasing k is to decrease α_k. Thus $\frac{dI_u}{dk}$ has the opposite sign of $\frac{dI_u}{d\alpha_k}$. Note that since (5.10) and (5.11) have the same form as (5.1) and (5.2), the result follows from the proof of Proposition 5.1. ■

Remark 5.4. We noted previously that in networks with no cells in common, for sufficiently large n the transition from fusion will be to WTA and not rivalry. Since increasing k has the

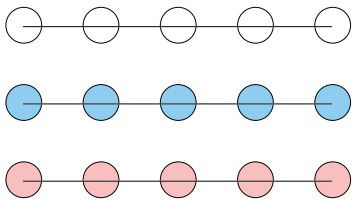

Figure 11. *Three patterns with no cells pairwise in common.*

effect of decreasing α_k, it can recover the possibility of transitions from fusion to rivalry in such networks with large n. We can see this by again considering (5.6), the condition that dictates when Hopf bifurcation from the synchronous equilibrium occurs before steady-state branching. ■

6. Discussion and future directions. We are still far from a complete understanding of the dynamics present in Wilson's generalized rivalry model. A systematic comparison of the model dynamics and experimental features of rivalry, such as Levelt's propositions characterizing perceptual dominance durations as a function of image contrasts (Levelt (1965)), would be instructive. In this concluding section we comment on three mathematical issues: transverse bifurcations, three learned patterns, and many learned patterns.

Transverse bifurcations. Our analysis does not preclude a bifurcation whose critical eigenvectors are transverse to $\mathcal{S}$, at least when (2.1) fails. Preliminary calculations show that such bifurcations cannot take place from a stable fusion state, but they may well occur from a stable WTA state. It is surely the case that $\mathcal{S}$ is not always locally attracting on all of $\mathcal{S}$.

Three learned patterns. Rivalry between two learned patterns is the simplest case of generalized rivalry. In this paper, we showed how the number of cells in common to two learned patterns changes the (effective) recurrent excitation in associated quotient two- and three-cell systems. Our methods can help analyze an arbitrary number of patterns; however, when there are more than two learned patterns, the number of ways in which the structure of the connections between the patterns can occur becomes large fast and each leads to a different type of quotient network. For three learned patterns there are nine classes of quotient networks, rather than the two in the two-pattern case. We note that Naber, Gruenhage, and Einhäuser (2010) present evidence for rivalry among three patterns.

Wilson (2009) has considered three learned patterns and found parameter values that exhibit rivalry among the three patterns. The simplest case is when the three learned patterns have no cells in common, as in Figure 11, where nodes of the same color are active in the same pattern. In this case, the quotient network is a three-cell bidirectional ring with reciprocal inhibition between cells, apparent recurrent excitation in each cell, and S_3 symmetry. We believe that the existence of symmetry-breaking TB points will provide us with a way to study the detailed dynamics in three-pattern quotient networks. In this case the bifurcation of interest will be an $\mathbf{S}_3$ symmetry-breaking TB bifurcation—one that has not previously been studied.

At the other extreme, the most complicated case of three learned patterns in a 5-attribute 3–intensity level system is illustrated in Figure 12, where the cells marked by the same line are active in the same pattern. In this case, all patterns have the same intensity level in attribute

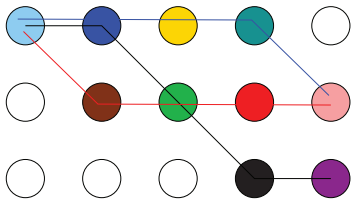

Figure 12. *Each pair of patterns has common active cells.*

1, all patterns have different intensity levels in attribute 4, and the patterns have intensity levels pairwise in common in attributes $2, 3, 5$ (with different pairs). Also, in this case, the quotient network and the network with inactive cells removed are identical, and each has 10 nodes. There are three nodes that correspond to the attribute with no cells in common; there are six nodes that correspond to attributes that have two patterns having cells in common (one node for each pair and one node for each singleton); and there is one node corresponding to the attribute having all cells in common. For an n-attribute m–intensity level system, the most complicated case with three learned patterns is similar to the 5×3 case. Although the number of cells in each color may be greater than one, there is still a 10-cell quotient network. Simulations show that cells of the same color are synchronous, and we expect that the dynamics will reduce to the 10-cell quotient system.

How many patterns can a generalized network support? Wilson raises the question that titles this subsection. He finds in simulations that the number is rather small in the sense that rivalry predominates in simulations when the system has learned four or five different patterns in his 5-attribute 3–intensity level system. In principle, an n-attribute m–intensity level system could learn m^n different patterns (or 243 patterns in the working example). However, it does seem likely that the resulting dynamics would settle into a rivalry with cycling between different patterns should the network have learned all possible patterns. Although no reduction is possible in this extreme case (all cells are active), it may still be a tractable analysis because of the huge symmetry group, the wreath product group $S_m \wr S_n$ with $(m!)^n n!$ elements (or 933120 symmetries in the working example). It is also known that wreath product symmetric coupled cell systems often lead to heteroclinic cycles (or networks) on loss of stability of a symmetric (fusion) state. Indeed, the first example of a symmetry generated heteroclinic cycle (Guckenheimer and Holmes (1988)) has a wreath product symmetry group $\mathbf{Z}_2 \wr \mathbf{Z}_3$ (cf. Dionne, Golubitsky, and Stewart (1996)).

Acknowledgments. The authors thank Hugh Wilson for introducing them to rivalry networks, and Pete Ashwin and Claire Postlethwaite for useful discussions.

REFERENCES

R. Blake and N. K. Logothetis (2002), *Visual competition*, Nat. Rev. Neurosci., 3, pp. 13–21.
R. Blake and H. Wilson (2011), *Binocular vision*, Vision Res., 51, pp. 754–770.
G. Burton (2002), *Successor states in a four-state ambiguous figure*, Psychon. Bull. Rev, 9, pp. 292–297.
R. Curtu (2010), *Singular Hopf bifurcations and mixed-mode oscillations in a two-cell inhibitory neural network*, Phys. D, 239, pp. 504–514.

R. Curtu, A. Shpiro, N. Rubin, and J. Rinzel (2008), *Mechanisms for frequency control in neuronal competition models*, SIAM J. Appl. Dyn. Syst., 7, pp. 609–649.
B. Dionne, M. Golubitsky, and I. Stewart (1996), *Coupled cells with internal symmetry.* I. *Wreath products*, Nonlinearity, 9, pp. 559–574.
M. Golubitsky and D. G. Schaeffer (1985), *Singularities and Groups in Bifurcation Theory,* Vol. I, Appl. Math. Sci. 51, Springer-Verlag, New York.
M. Golubitsky and I. Stewart (2006), *Nonlinear dynamics of networks: The groupoid formalism*, Bull. Amer. Math. Soc. (N.S.), 43, pp. 305–364.
M. Golubitsky, I. Stewart, and D. G. Schaeffer (1988), *Singularities and Groups in Bifurcation Theory,* Vol. II, Appl. Math. Sci. 69, Springer-Verlag, New York.
M. Golubitsky, I. Stewart, and A. Török (2005), *Patterns of synchrony in coupled cell networks with multiple arrows*, SIAM J. Appl. Dyn. Syst., 4, pp. 78–100.
J. Guckenheimer and P. Holmes (1983), *Nonlinear Oscillations, Dynamical Systems, and Bifurcations of Vector Fields*, Appl. Math. Sci. 42, Springer-Verlag, New York.
J. Guckenheimer and P. Holmes (1988), *Structurally stable heteroclinic cycles*, Math. Proc. Cambridge Philos. Soc., 103, pp. 189–192.
Z. P. Kilpatrick and P. C. Bressloff (2010), *Binocular rivalry in a competitive neural network with synaptic depression*, SIAM J. Appl. Dyn. Syst., 9, pp. 1303–1347.
C. Laing and C. Chow (2001), *Stationary bumps in networks of spiking neurons*, Neural Comput., 13, pp. 1473–1494.
C. Laing and C. Chow (2002), *A spiking neuron model for binocular rivalry*, J. Comput. Neurosci., 12, pp. 39–53.
W. J. M. Levelt (1965), *On Binocular Rivalry*, Institute for Perception RVO-TNO, Soesterberg, The Netherlands.
S. Moldakarimov, J. E. Rollenhagen, C. R. Olson, and C. C. Chow (2005), *Competitive dynamics in cortical responses to visual stimuli*, J. Neurophysiol., 94, pp. 3388–3396.
J. Montaldi (1994), *The path formulation of bifurcation theory*, in Dynamics, Bifurcations and Symmetry, NATO Adv. Sci. Inst. Ser. C Math. Phys. Sci. 437, P. Chossat, ed., Kluwer, Dordrecht, The Netherlands.
R. Moreno-Bote, J. Rinzel, and N. Rubin (2007), *Noise-induced alternations in an attractor network model of perceptual bistability*, J. Neurophysiol., 98, pp. 1125–1139.
M. Naber, G. Gruenhage, and W. Einhäuser (2010), *Tri-stable stimuli reveal interactions among subsequent percepts: Rivalry is biased by perceptual history*, Vision Res., 50, pp. 818–828.
J. Seely and C. C. Chow (2011), *The role of mutual inhibition in binocular rivalry*, J. Neurophysiol., 106, pp. 2136–2150.
A. Shpiro, R. Curtu, J. Rinzel, and N. Rubin (2007), *Dynamical characteristics common to neuronal competition models*, J. Neurophysiol., 97, pp. 462–473.
A. Shpiro, R. Moreno-Bote, N. Rubin, and J. Rinzel (2009), *Balance between noise and adaptation in competition models of perceptual bistability*, J. Comput. Neurosci., 27, pp. 37–54.
F. Takens (1974), *Forced oscillations and bifurcations*, in Applications of Global Analysis, I, Commun. Math. Inst. Rijksunivers. Utrecht 3, Math. Inst. Rijksuniv. Utrecht, Utrecht, The Netherlands, pp. 1–59.
A. L. Taylor, G. W. Cottrell, and W. B. Kristan, Jr. (2002), *Analysis of oscillations in a reciprocally inhibitory network with synaptic depression*, Neural Comput., 14, pp. 561–581.
F. Tong, M. Meng, and R. Blake (2006), *Neural bases of binocular rivalry*, Trends Cogn. Sci., 10, pp. 502–511.
R. van Ee (2009), *Stochastic variations in sensory awareness are driven by noisy neuronal adaptation: Evidence from serial correlations in perceptual bistability*, J. Opt. Soc. Am. A Opt. Image Sci. Vis., 26, pp. 2612–2622.
H. Wilson (2003), *Computational evidence for a rivalry hierarchy in vision*, Proc. Natl. Acad. Sci. USA, 100, pp. 14499–14503.
H. Wilson (2007), *Minimal physiological conditions for binocular rivalry and rivalry memory*, Vision Res., 47, pp. 2741–2750.
H. Wilson (2009), *Requirements for conscious visual processing*, in Cortical Mechanisms of Vision, M. Jenkin and L. Harris, eds., Cambridge University Press, New York, pp. 399–414.
H. Wilson (2012), *Binocular rivalry: Cooperation, competition, and decisions*, in The Constitution of Visual Consciousness: Lessons from Binocular Rivalry, Adv. in Consciousness Res. (AiCR), S. M. Miller, ed., John Benjamins Publishing, Amsterdam, to appear.